

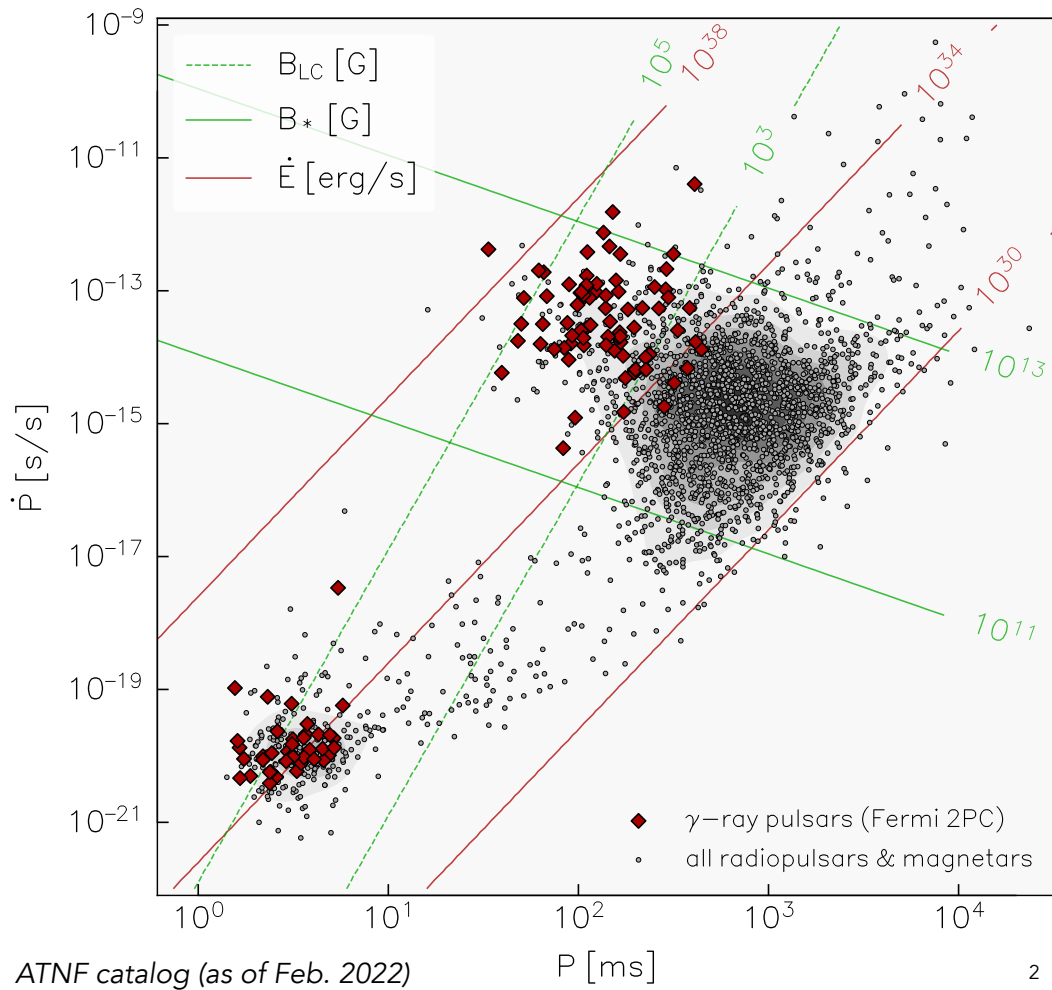
# ENERGY DISSIPATION AND EMISSION IN GAMMA-RAY PULSARS

ANATOLY SPITKOVSKY (PRINCETON)  
HAYK HAKOBYAN (PPPL/PRINCETON/COLUMBIA)  
SASHA PHILIPPOV (UMD)

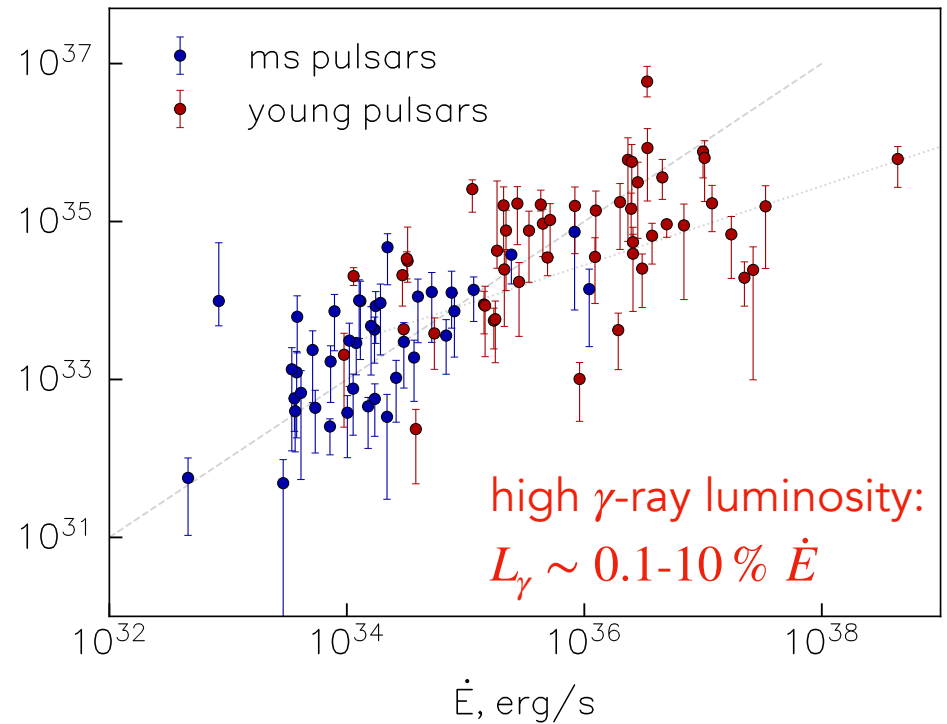
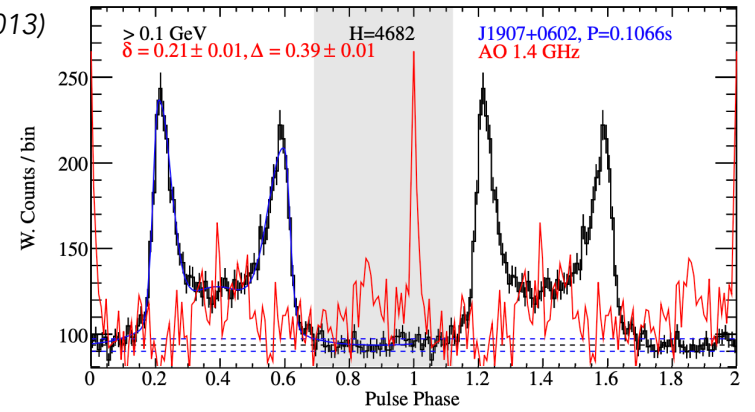
Hakobyan, Philippov, AS 22  
arXiv:2209.02121

# Observations

Fermi data: Abdo+ (2013) 2nd Pulsar Catalog



Abdo+ (2013)

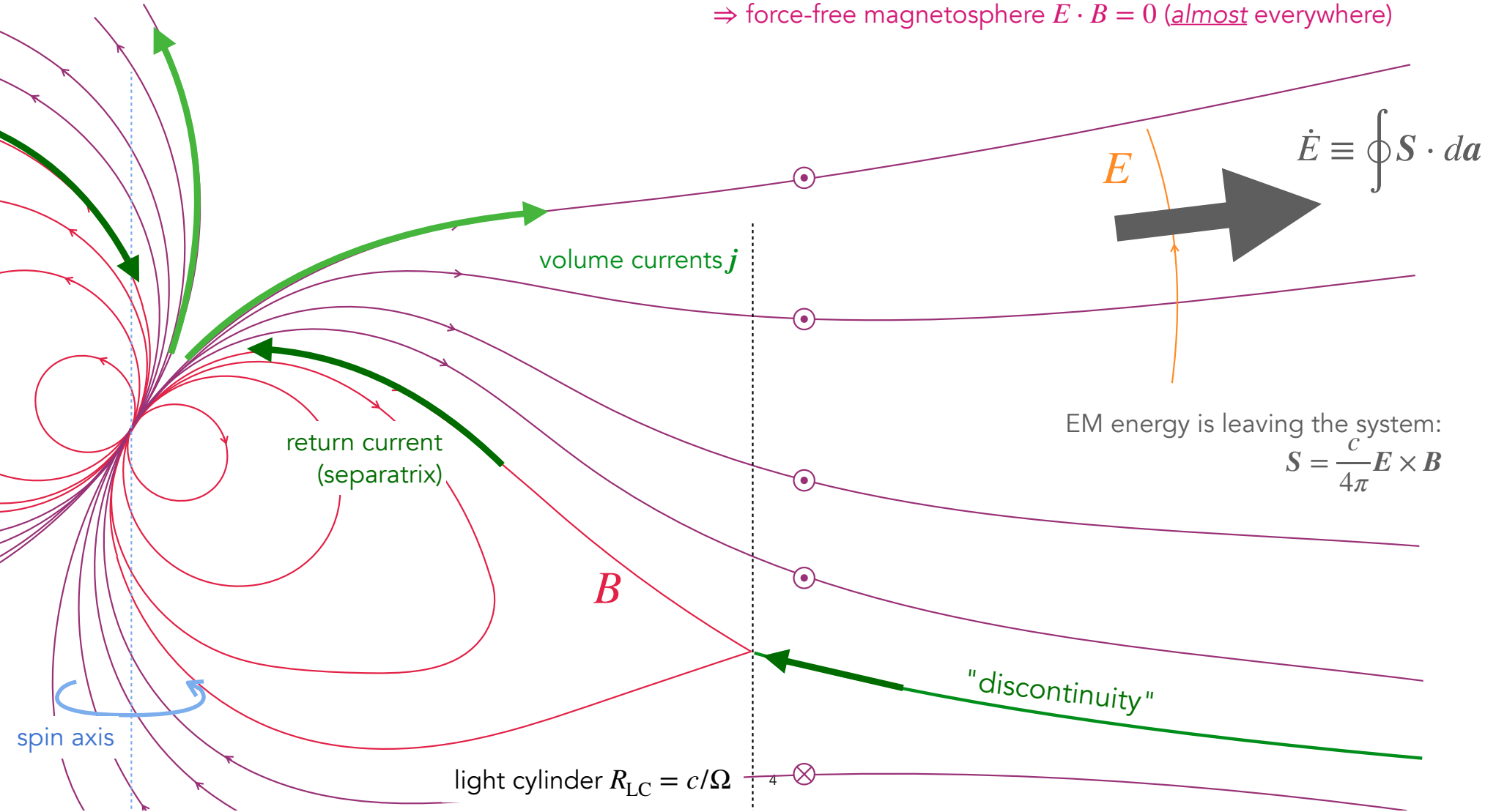


## Plan

1. What is different between high and low  $L_\gamma/\dot{E}$  pulsars?
2. Physics of energy dissipation.
3. Physics of particle energization and radiation.
4. Something completely different...

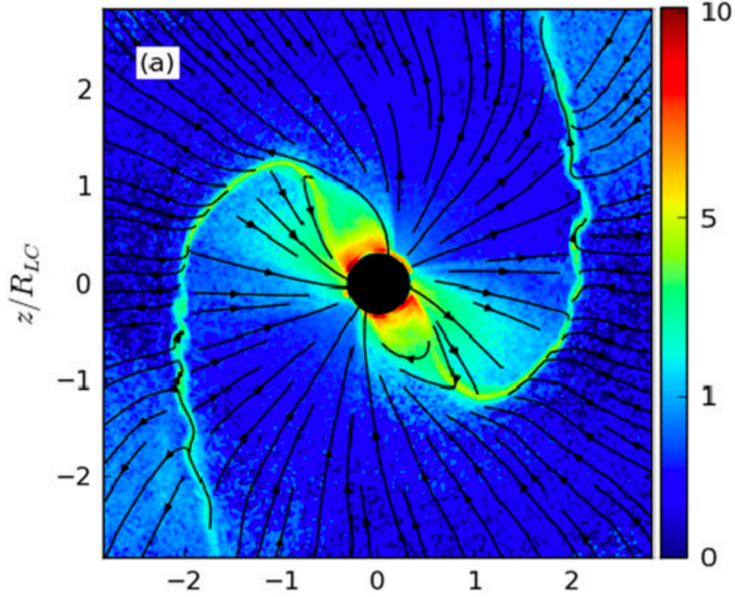
# Magnetospheres of pulsars

Magnetospheres of *Fermi* pulsars are filled with abundant pair plasma:  $n_{e\pm} \gg \rho_{GJ}/|e|$ .  
 $\Rightarrow$  force-free magnetosphere  $E \cdot B = 0$  (almost everywhere)

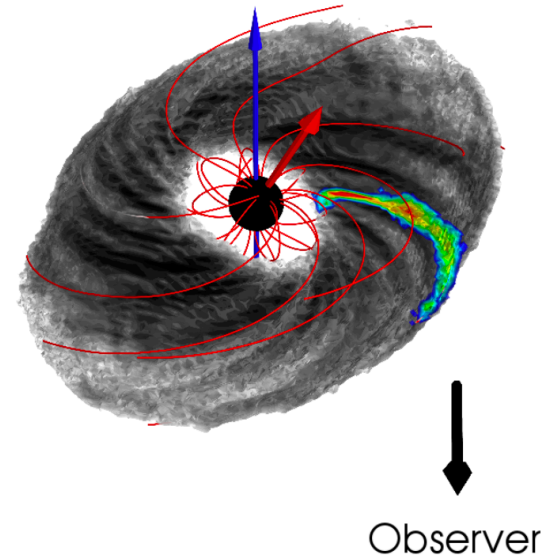
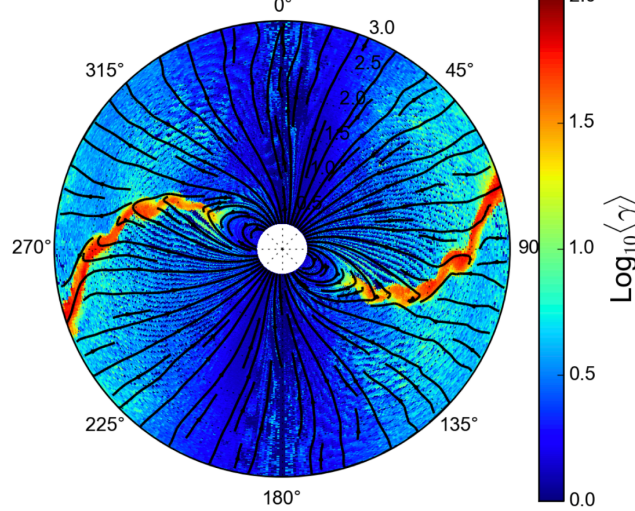


# Magnetospheres of pulsars (PIC simulations)

Electron density



Positrons



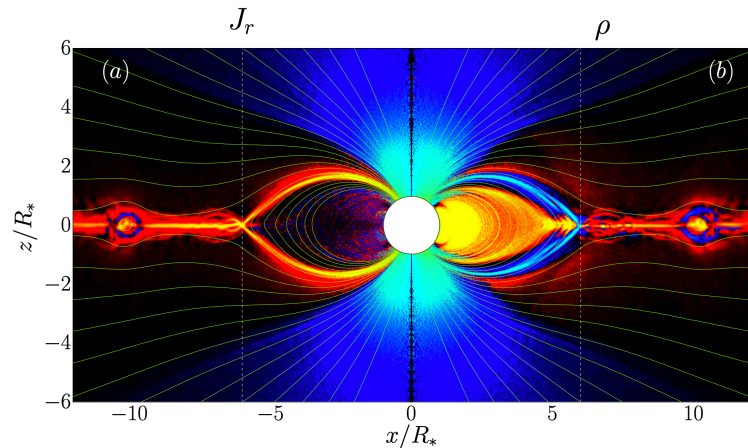
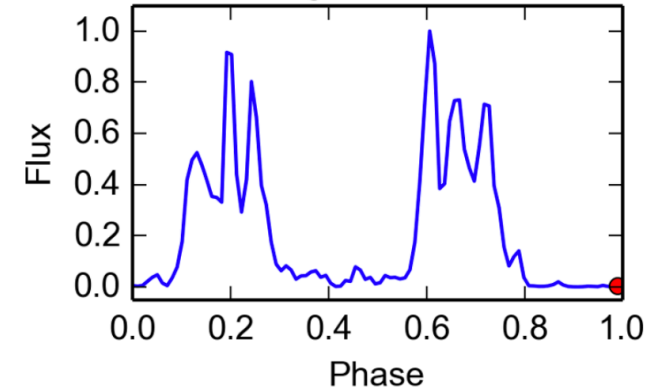
"discontinuity" = current sheet

width of the layer is microscopic!

$$d_e = c/\omega_{pe} \lll R_{LC}$$

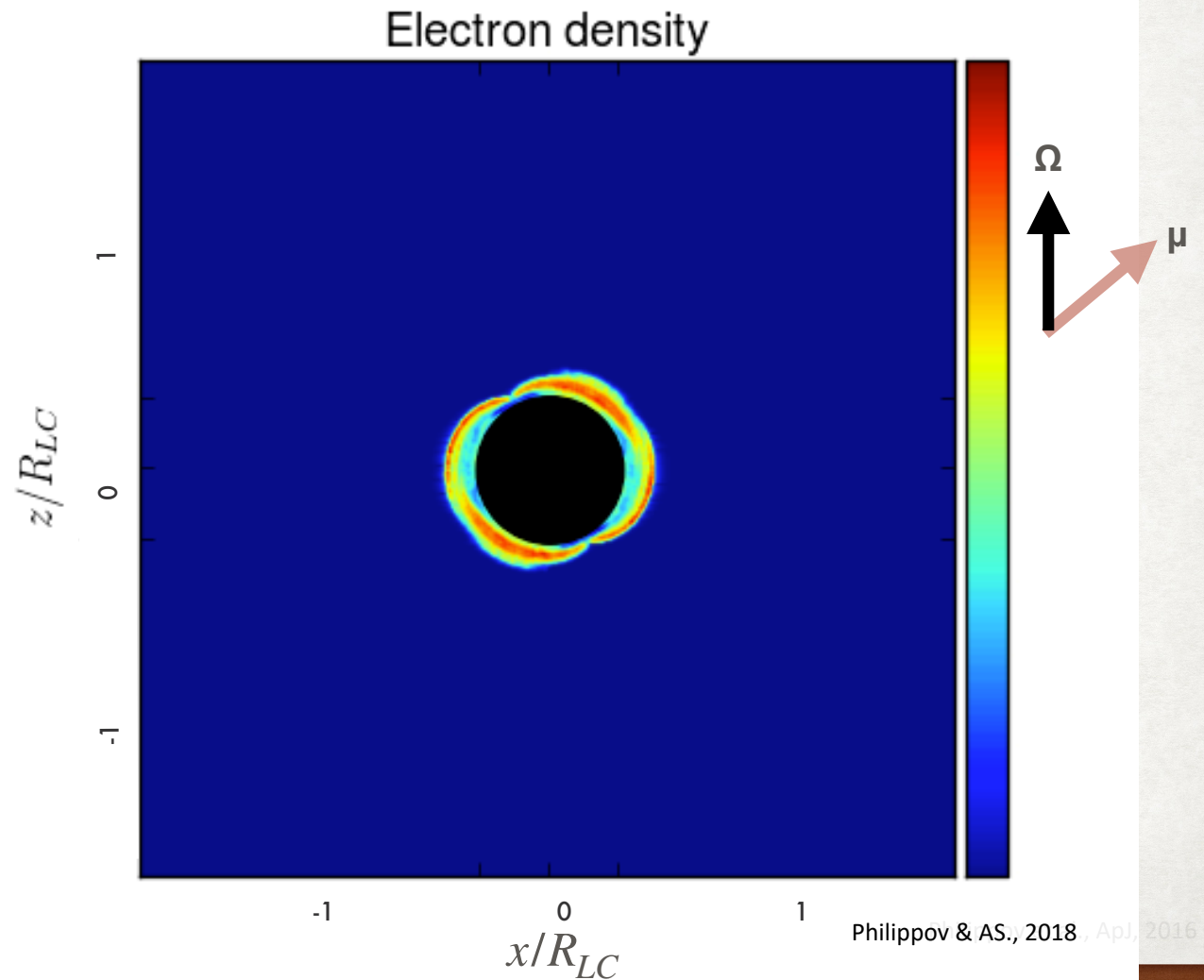
- Philippov, Spitkovsky (2014-2018)
- Chen, & Beloborodov (2014)
- Cerutti, et al. (2016+)
- Belyaev (2015)
- Kalapotharakos, et al. (2018)
- Hu, & Beloborodov (2021)

Lightcurve

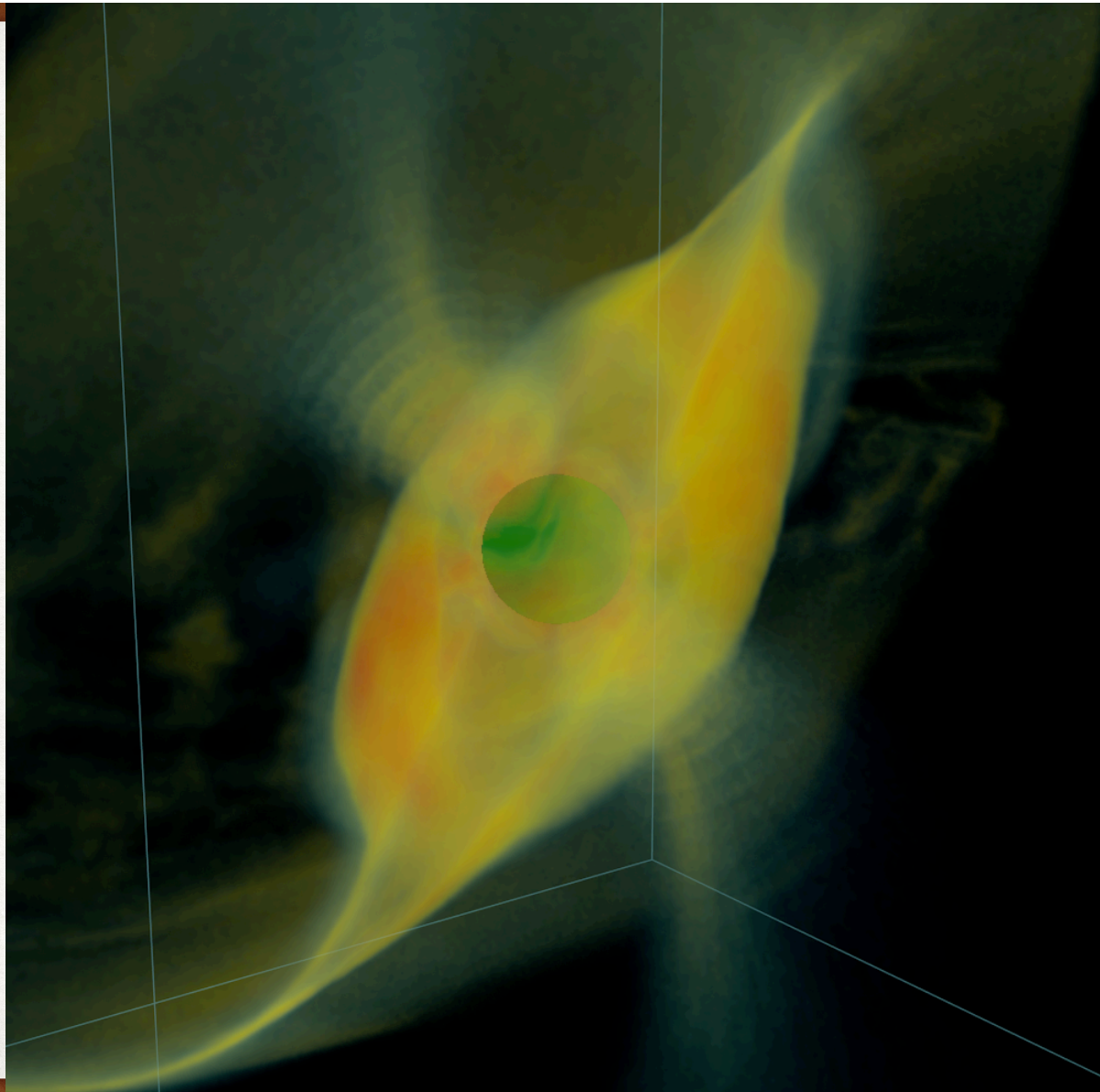


# OBLIQUE ROTATOR WITH GR AND PAIRS

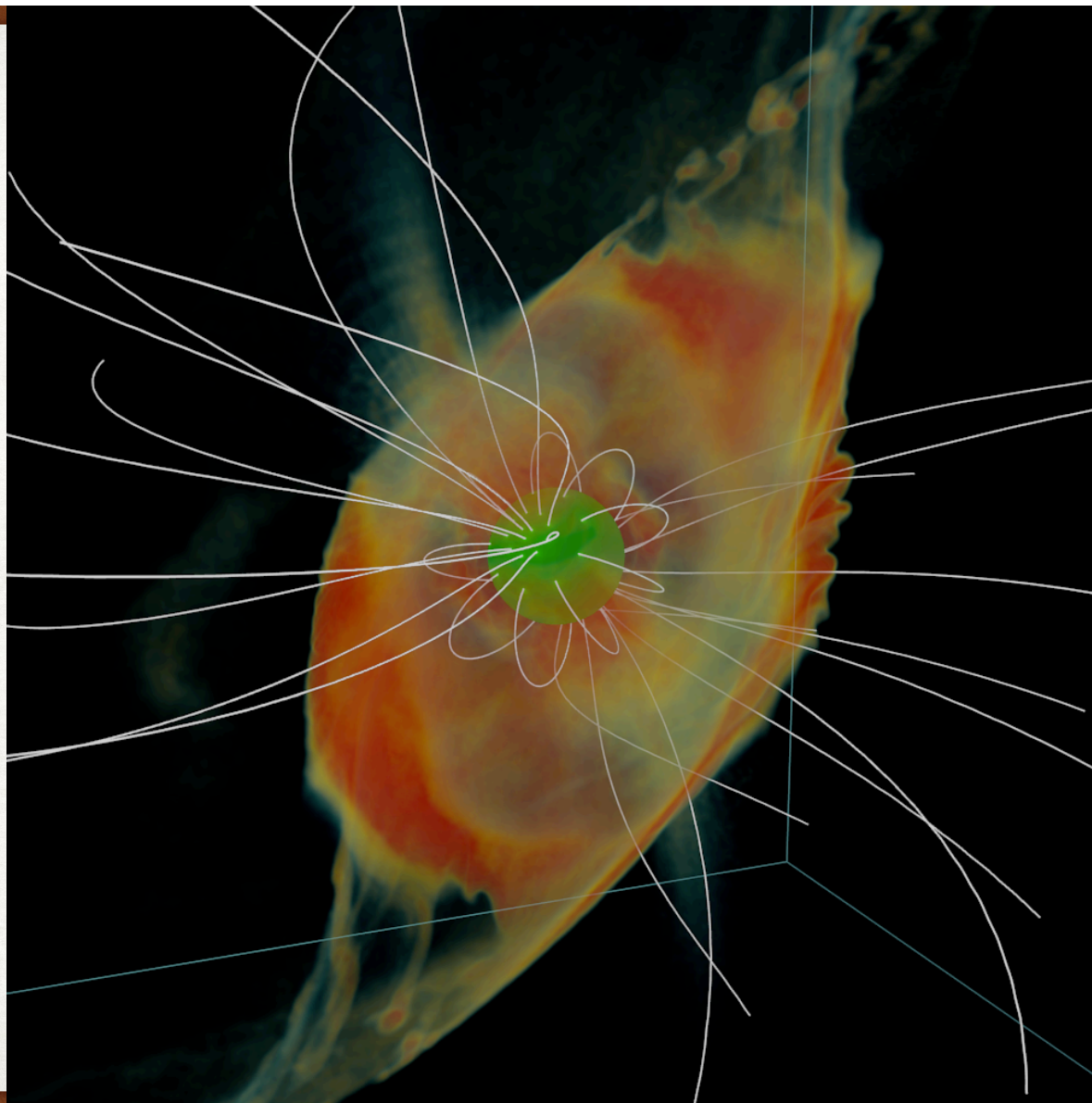
- Pair production happens on the polar cap, in return current layers and in the current sheet beyond LC
- Polar discharge is non-stationary. Electric field screening by advecting plasma clouds generates waves. The plasma motions are collective and coherent — implications for radio emission (see Beloborodov 2008, Timokhin & Arons 2013)



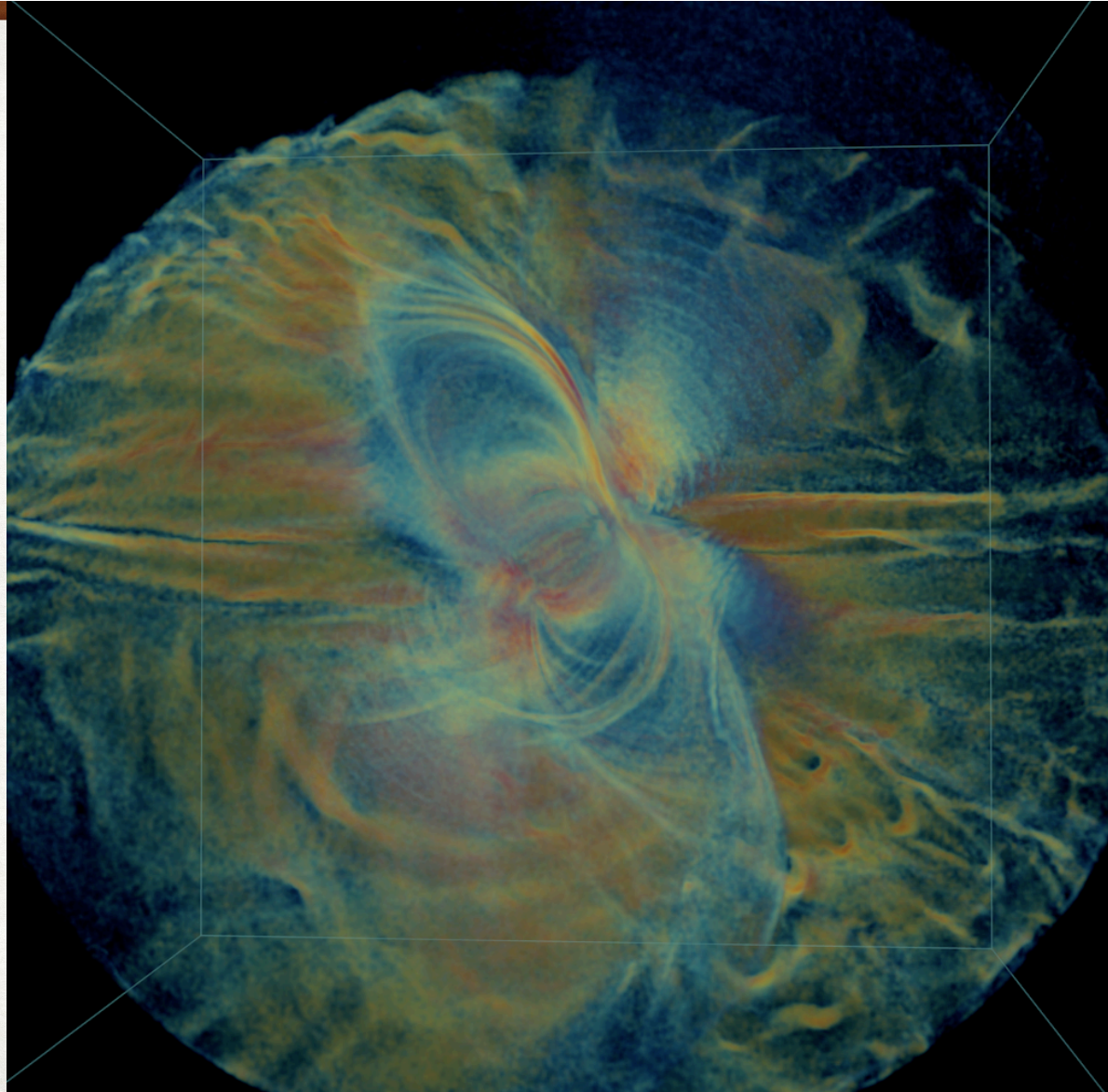
OBLIQUE  
ROTATOR WITH  
GR AND PAIRS:  
PLASMA DENSITY



OBLIQUE  
ROTATOR WITH  
GR AND PAIRS:  
PLASMA DENSITY



OBLIQUE  
ROTATOR WITH  
GR AND PAIRS:  
CURRENT DENSITY

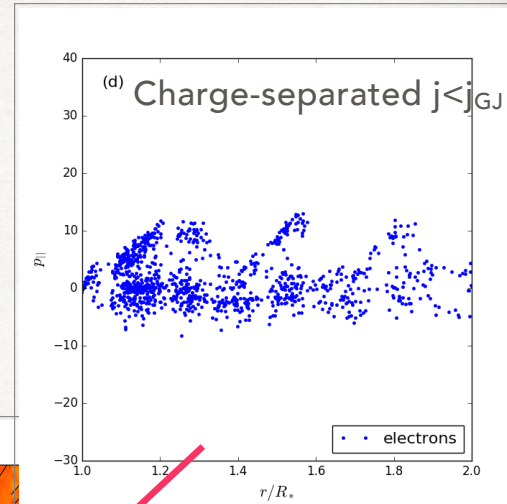
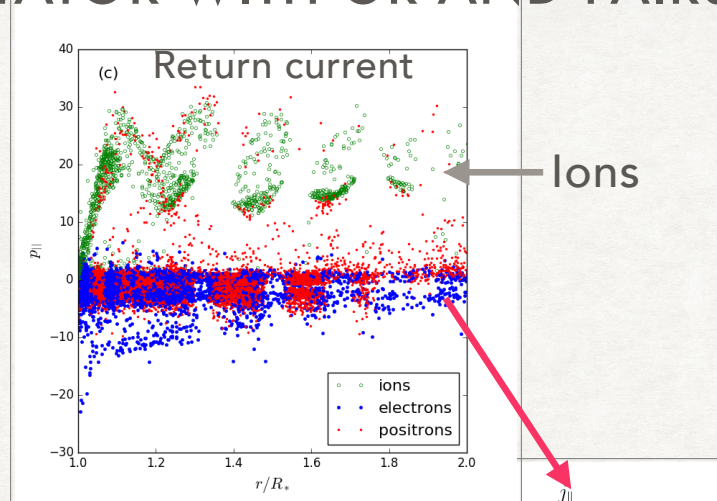


01, 2016

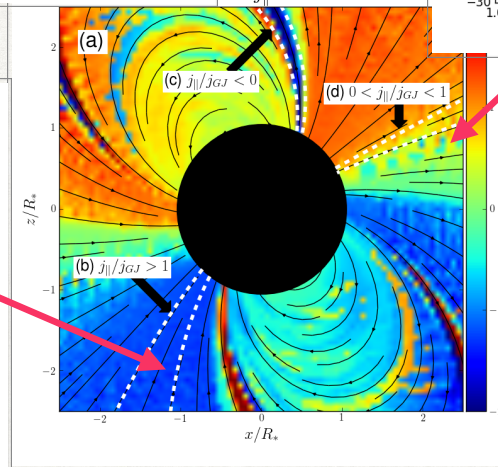
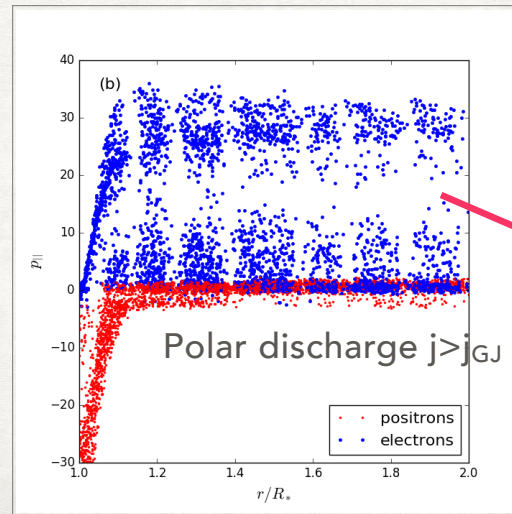
# OBLIQUE ROTATOR WITH GR AND PAIRS

- Counterstreaming is present in polar discharge and in return current region
- Opportunities for maser emission from collective instabilities of counterstreaming distributions.
- Also, time-dependent cascade

Momentum space

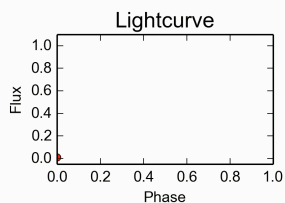
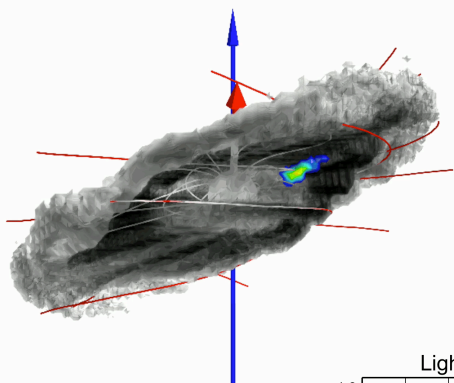


Accelerates ions!

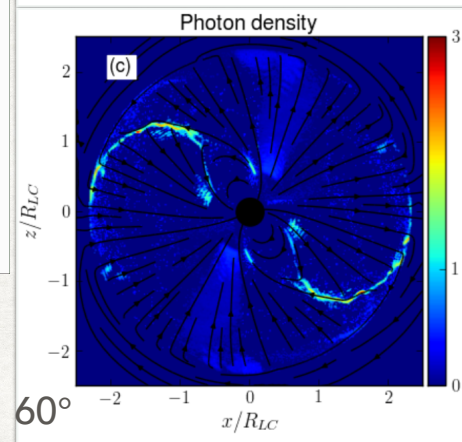
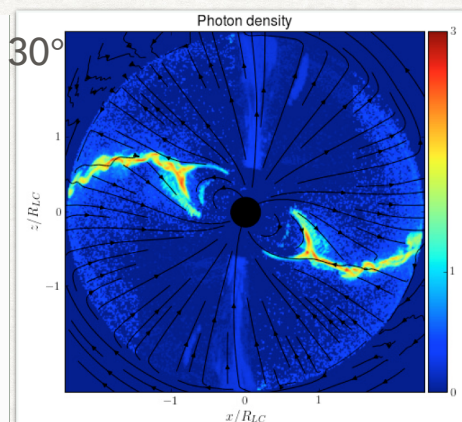


# GAMMA-RAY LIGHTCURVES

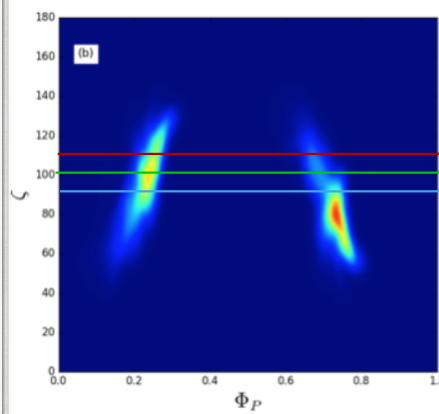
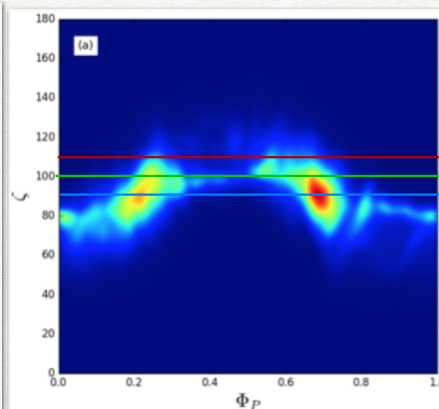
$i=30$  - Phase=0.00 - Positrons -



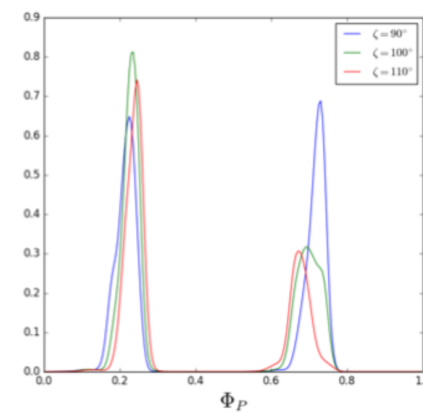
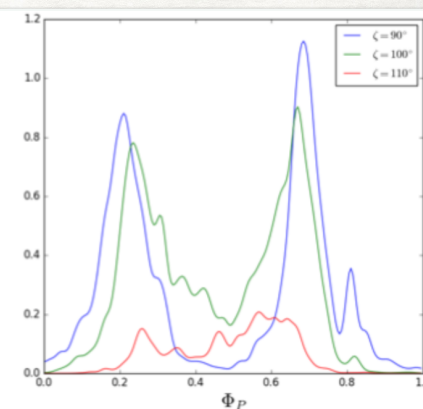
Caustic formation from spiral shape of current sheet



Photon density

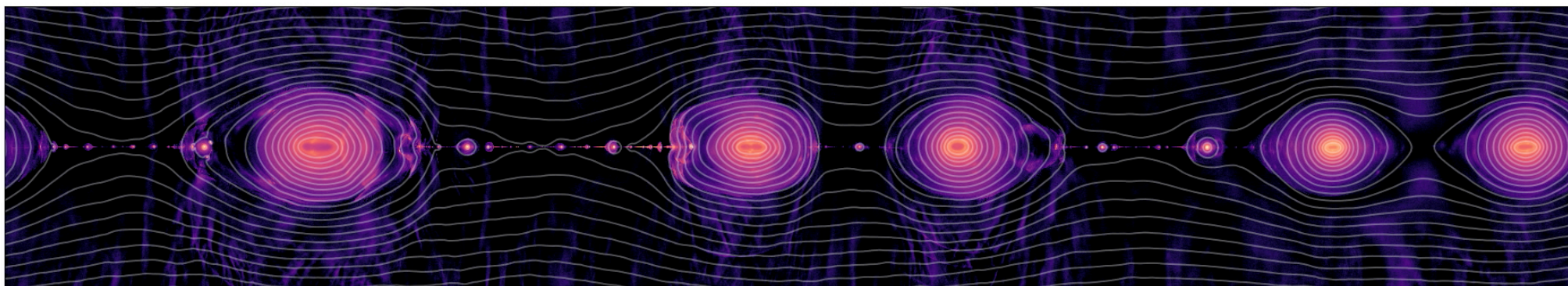


Sky map



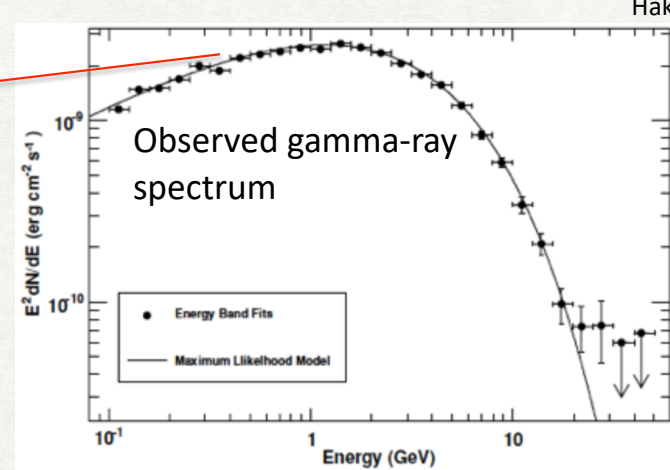
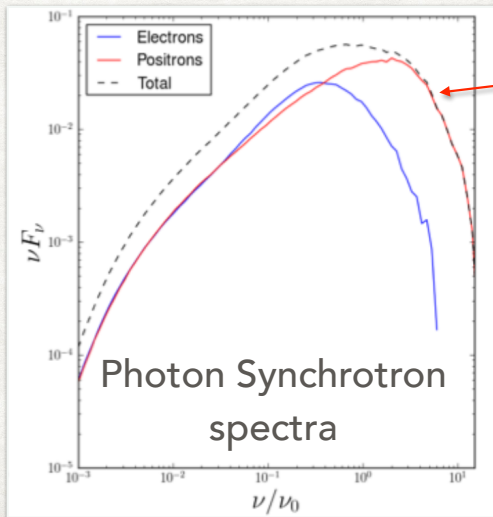
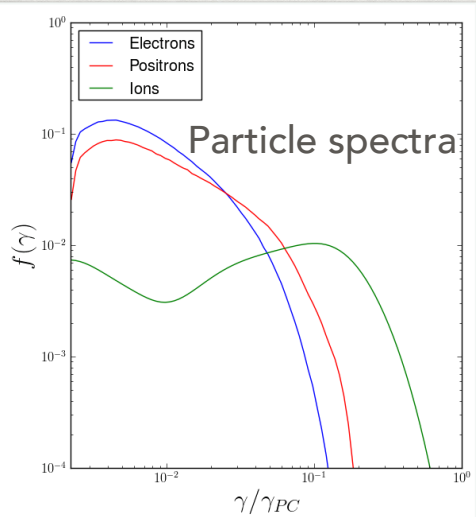
Light Curve

# PARTICLE ACCELERATION AND SPECTRA



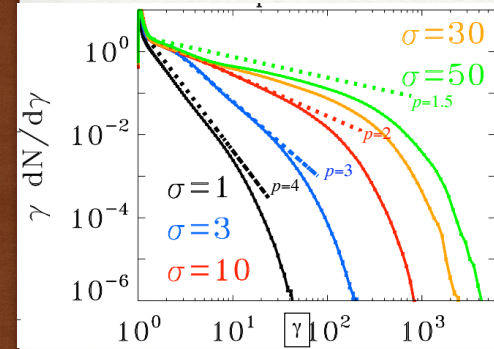
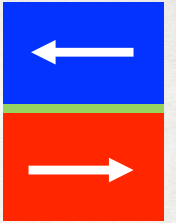
Magnetic reconnection results in particle acceleration

Hakobyan, Philippov, AS 2019



Pair production in the current sheet beyond light cylinder sets the peak emission frequency (Lund et al., ApJ, 2016)

# PARTICLE ACCELERATION IN RECONNECTION

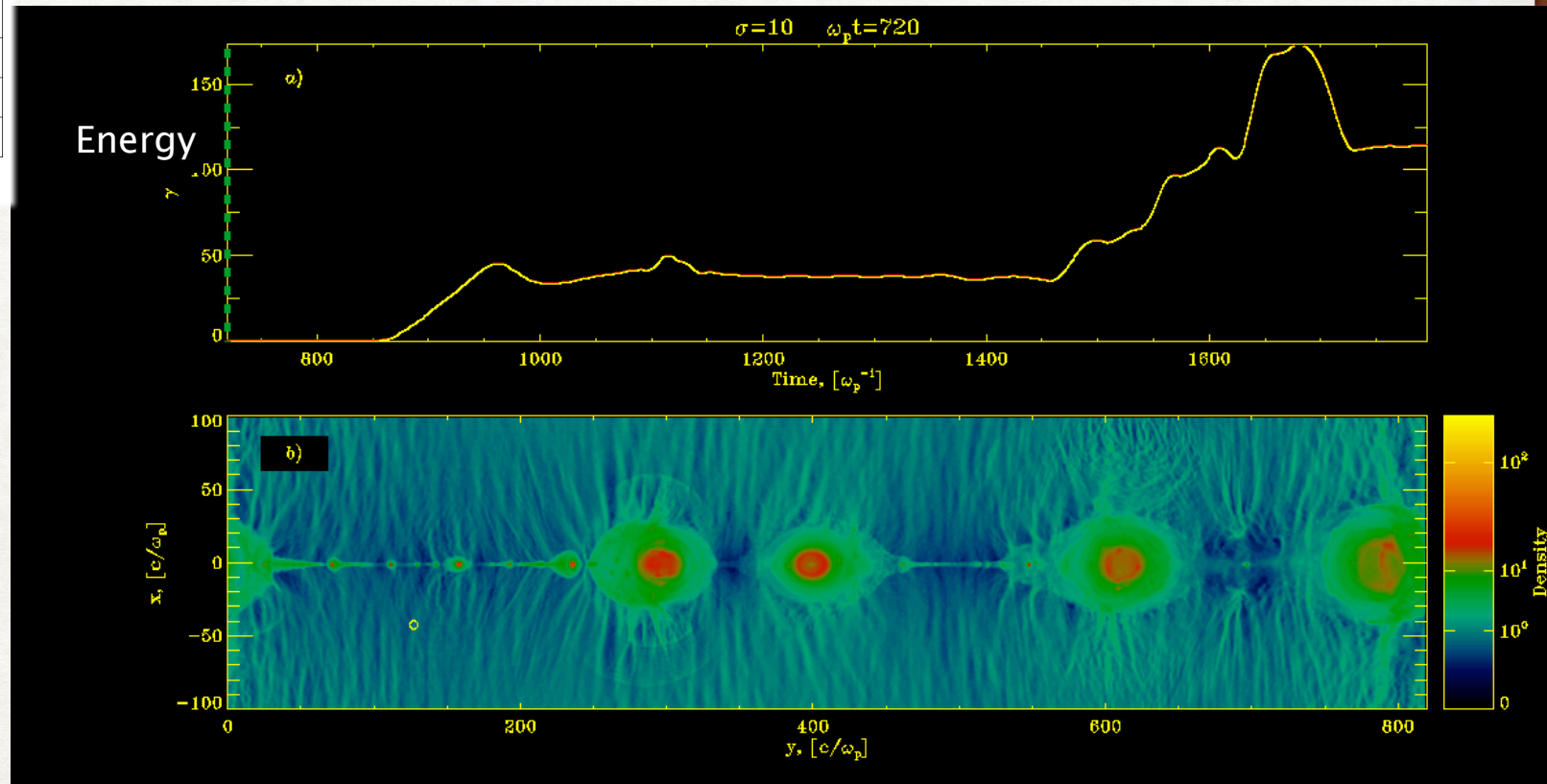


(Sironi & AS 14, Guo et al. 14, Werner et al. 14)

Relativistic reconnection produces extended non-thermal tails of accelerated particles, whose power-law slope is harder than  $p=2$  for high magnetizations ( $\sigma > 10$ )

Magnetization:

$$\sigma = \frac{B^2}{4\pi n m c^2}$$



Two acceleration phases: 1) at the X-point; 2) in between merging islands

# PARTICLE ACCELERATION AND SPECTRA

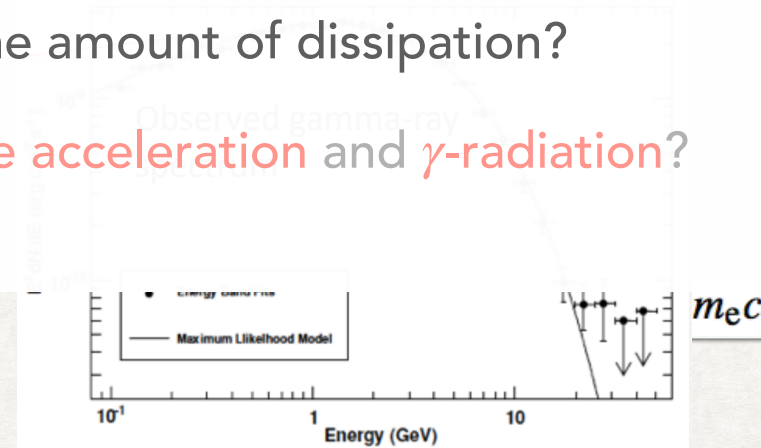
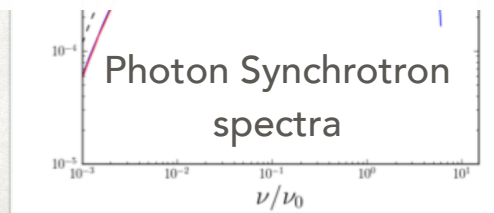
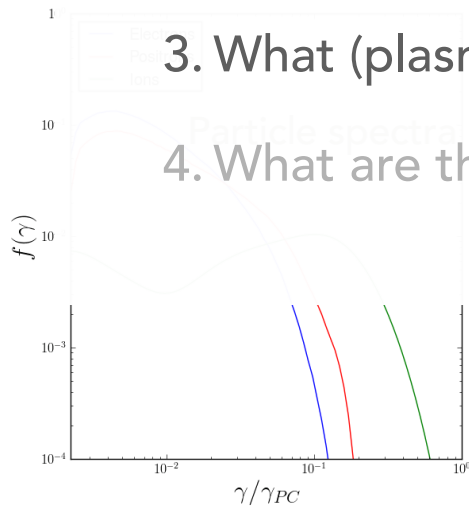
## Outstanding questions

1. What does the **microscopic dynamics** of the current layer look like?

2. **How much energy** is being dissipated within a few  $R_{LC}$ ?

3. What (plasma) **parameters** control the amount of dissipation?

4. What are the implications for **particle acceleration** and  $\gamma$ -radiation?



Pair production in the current sheet beyond light cylinder sets the peak emission frequency (Mikhailovskii et al., ApJ, 2016)

## Simulation setup

- injecting pairs *only near the surface* of the star (i.e., mimicking polar cap discharge)
- strong synchrotron cooling (near the LC):  
 $|e|E \sim \sigma_T \gamma^2 B$
- particles in the bulk of the magnetosphere (FF region) are treated as *Guiding Center Approximation*<sup>[\*]</sup> approach
- in the non-FF region (e.g.,  $E > B$ ) *full eq. of motion* is recovered

### real pulsars

$$R_{\text{LC}}/R_* \gtrsim 100$$

$$R_{\text{LC}}/d_e^{\text{LC}} \sim 10^8$$

$$n_{e\pm} \sim 10^4 - 10^6 n_{\text{GJ}}$$

$$\sigma^{\text{LC}} = \frac{2U_B^{\text{LC}}}{\rho_{e\pm} c^2} \sim 10^4 - 10^6$$

### "pulsars" in PIC

$$R_{\text{LC}}/R_* \sim 3-6$$

$$R_{\text{LC}}/d_e^{\text{LC}} \sim 100-200$$

$$n_{e\pm} \sim 10 n_{\text{GJ}}$$

$$\sigma^{\text{LC}} \sim 10^2 - 10^3$$

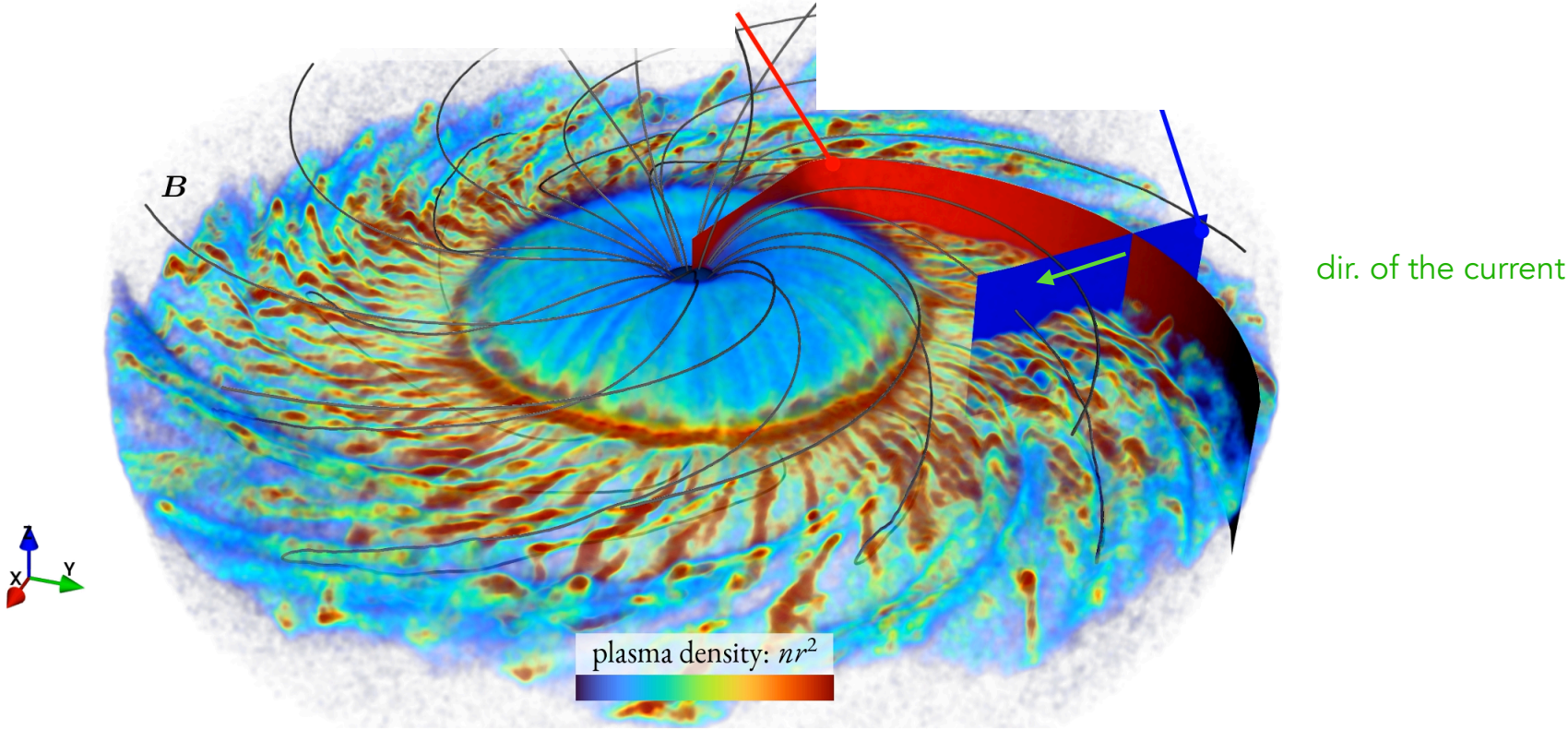
\*only the "accelerated" particles are shown

\*  $d_e^{\text{LC}} \sim 5$  cells

\* sizes of simulations:  
560<sup>3</sup>-2500<sup>3</sup> cells

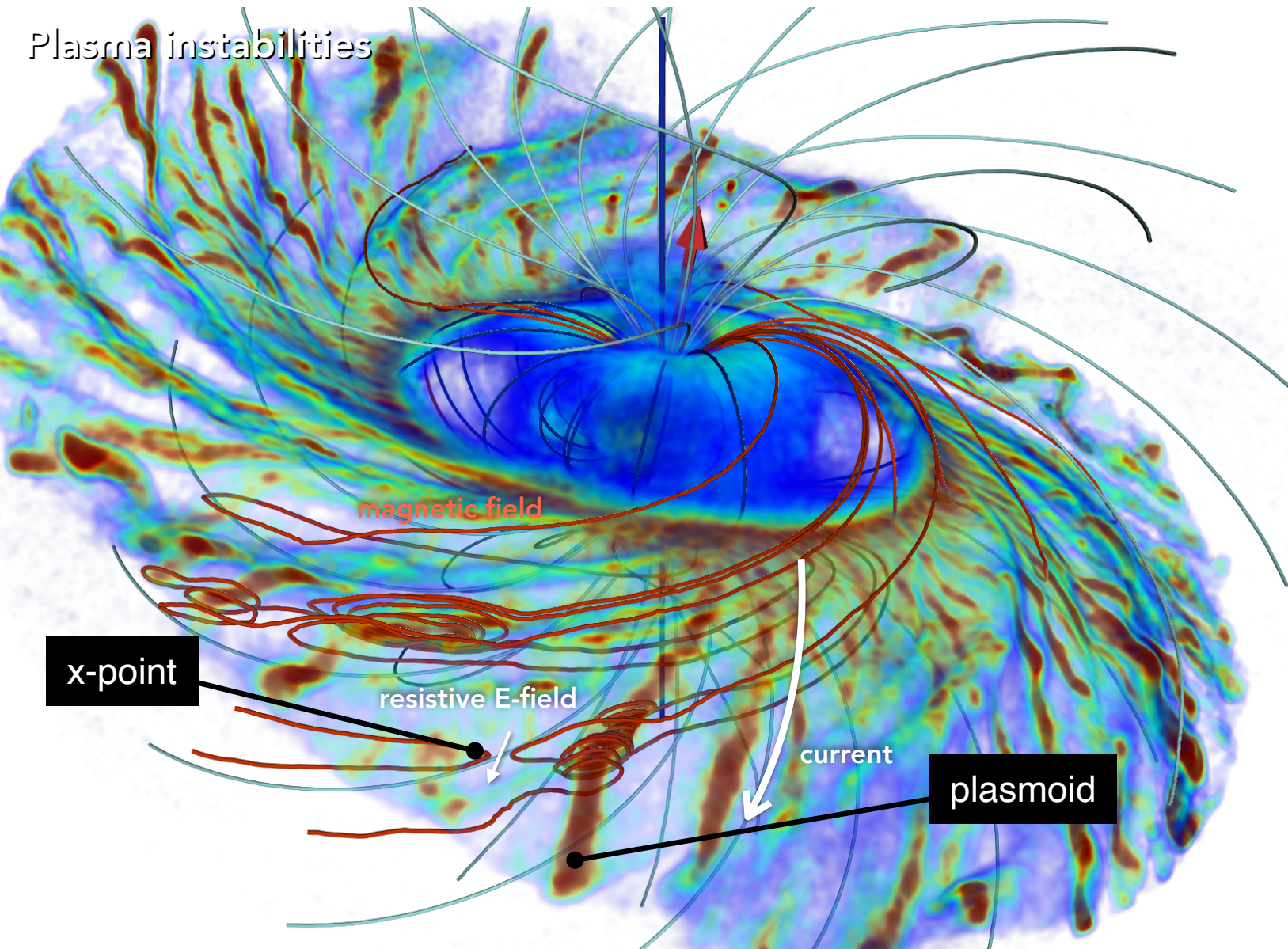
[\*] Bacchini, et al. (2020)

# Plasma instabilities



# Plasma instabilities

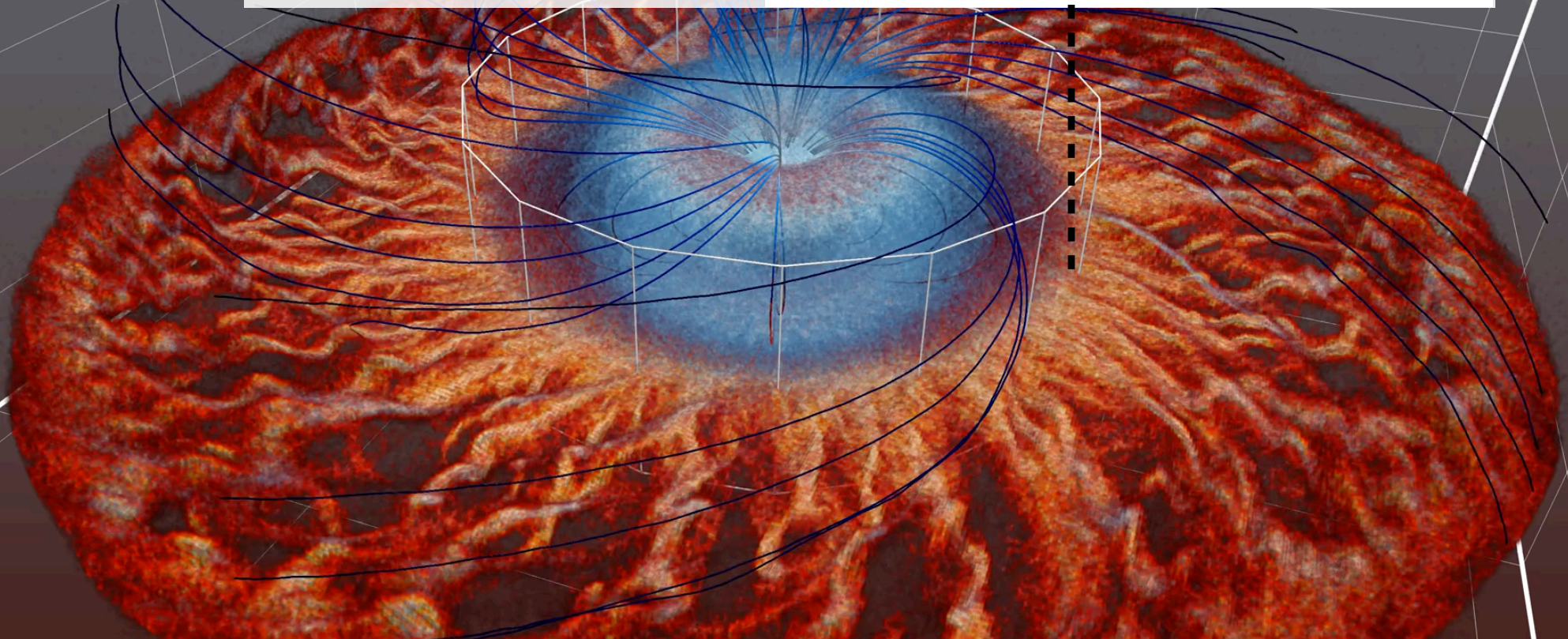
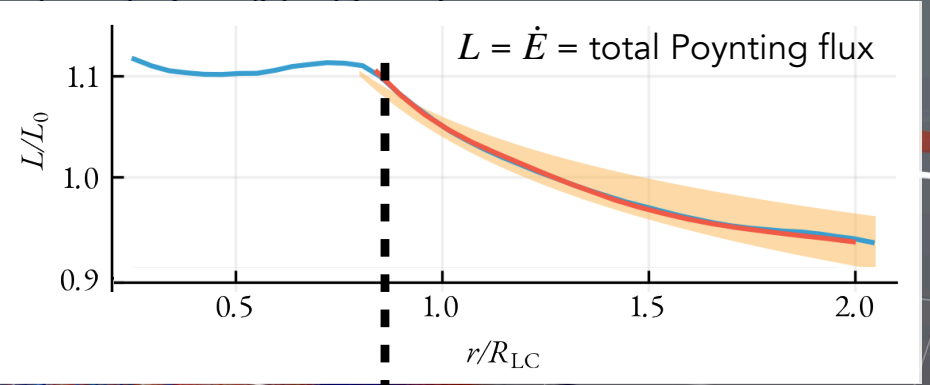
\* at larger inclinations  
drift-kink is less prominent



# Energy dissipation

Particle-in-cell simulation

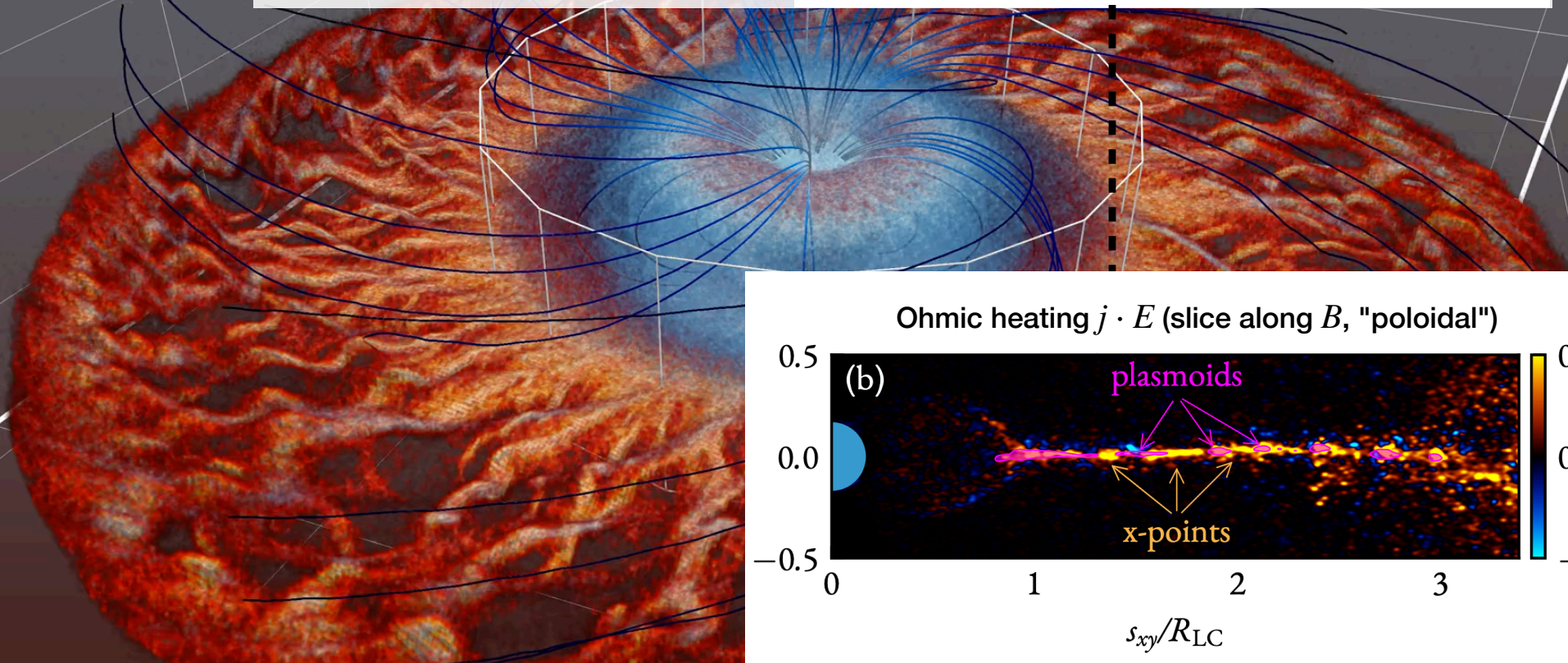
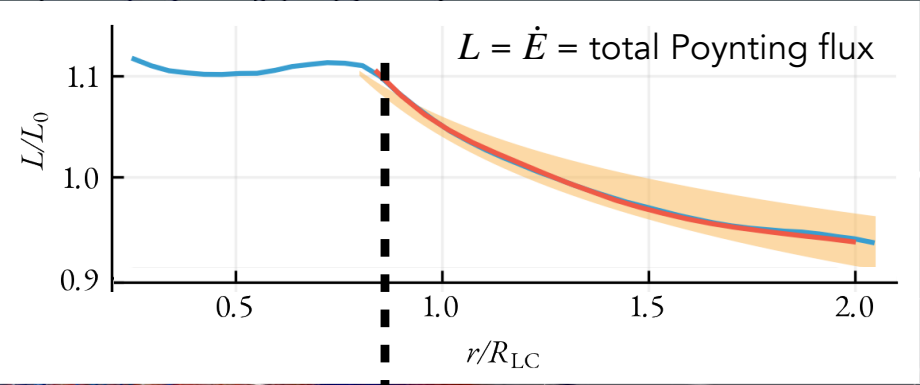
$\oint S_{da}$



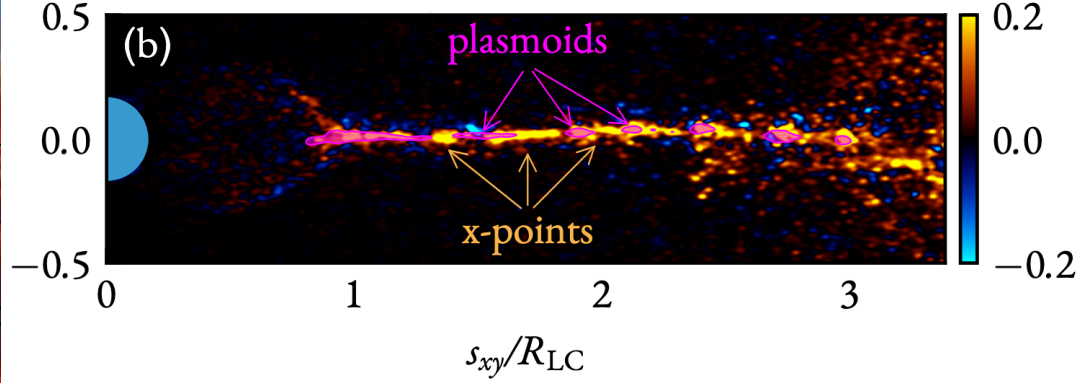
# Energy dissipation

Particle-in-cell simulation

- $\oint S da$
- $L_0 - \int \mathbf{j} \cdot \mathbf{E} d^3r$



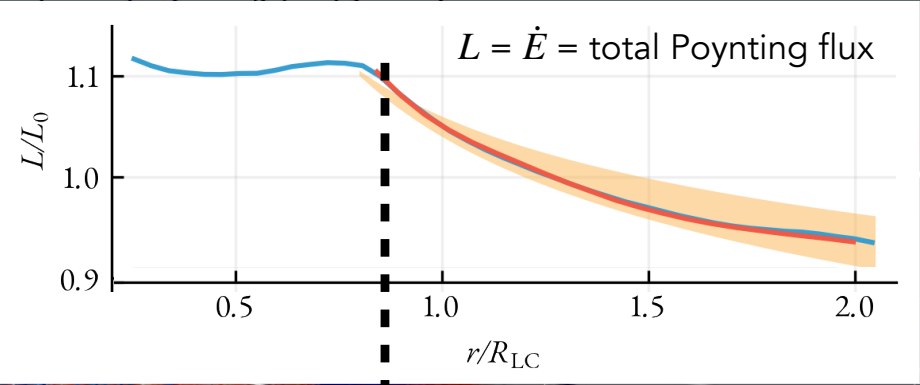
## Ohmic heating $\mathbf{j} \cdot \mathbf{E}$ (slice along $B$ , "poloidal")



# Energy dissipation

Particle-in-cell simulation

- $\oint S da$
- $L_0 - \int \mathbf{j} \cdot \mathbf{E} d^3r$
- $L_0 \left( 1 - \beta_{\text{rec}} \left[ \log \frac{r}{R_{\text{LC}}} + \frac{1}{2} \left( 1 - \left( \frac{r}{R_{\text{LC}}} \right)^{-2} \right) \right] \right)$

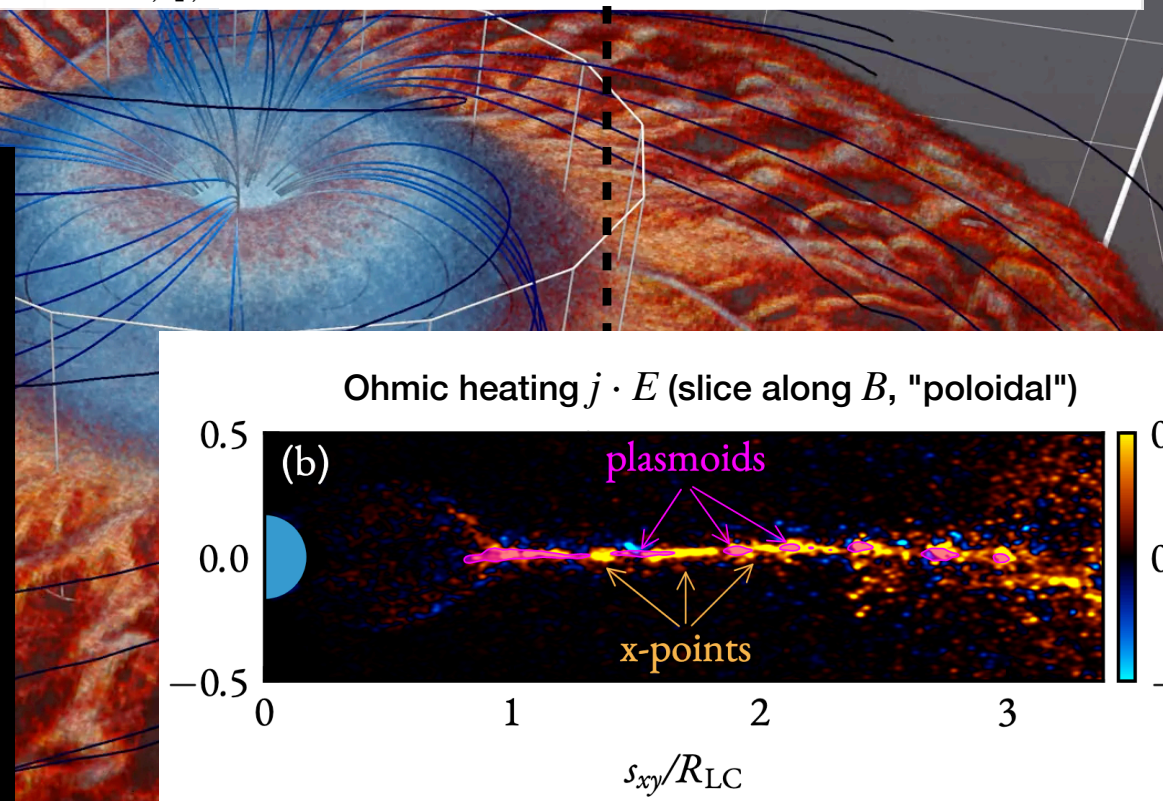


$$j \approx \nabla \times B \sim B/d_e \quad (d_e = c/\omega_{pe})$$

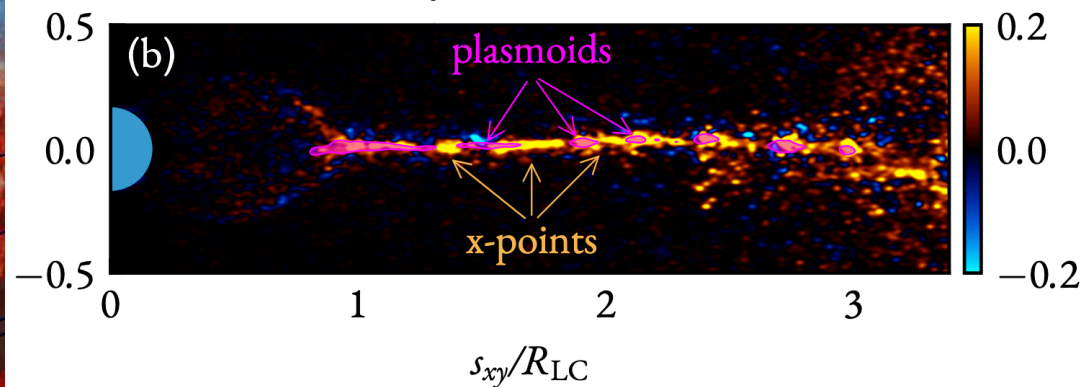
$$E \approx \beta_{\text{rec}} B, \quad B \sim \text{rotating monopole}$$

$$\Delta L = \int_{-d_e/2}^{d_e/2} d^3r (j \cdot E) \approx \beta_{\text{rec}} L_0 f(r/R_{\text{LC}})$$

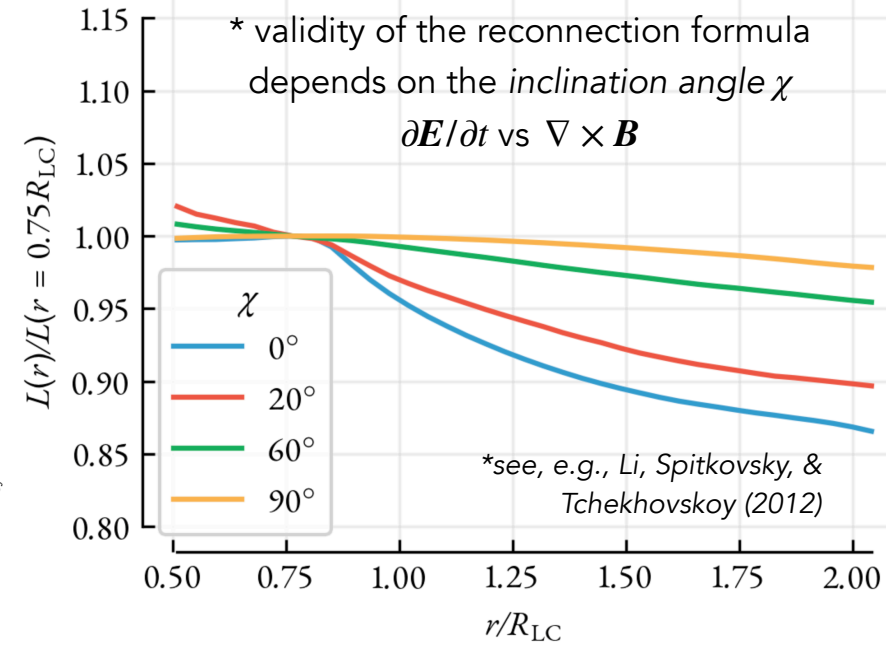
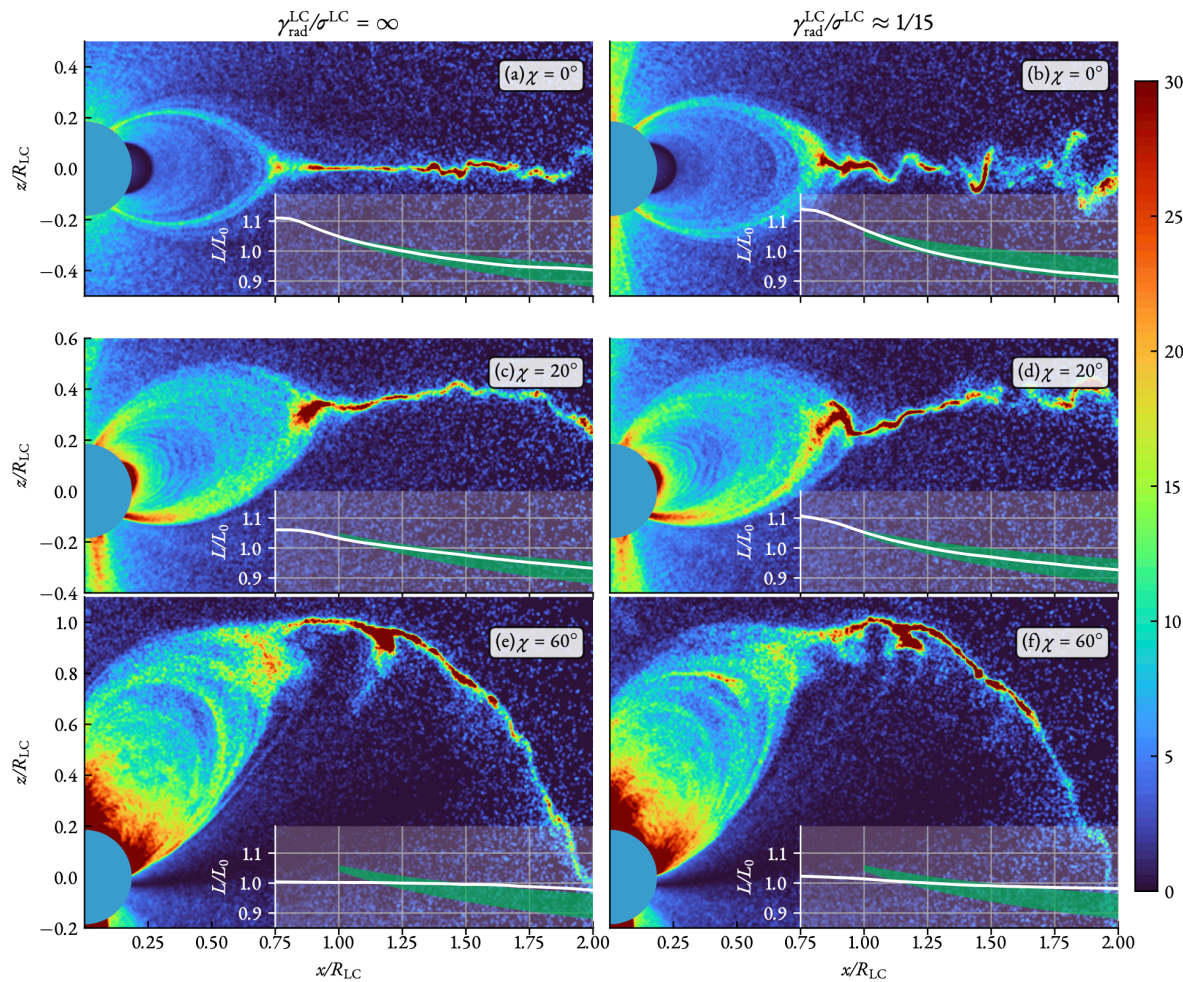
(see also Cerutti+ 2020 for  $\chi = 90^\circ$ )



Ohmic heating  $j \cdot E$  (slice along  $B$ , "poloidal")



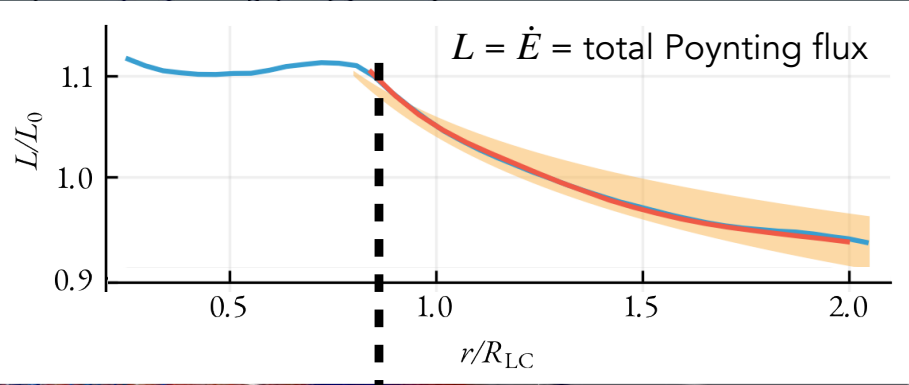
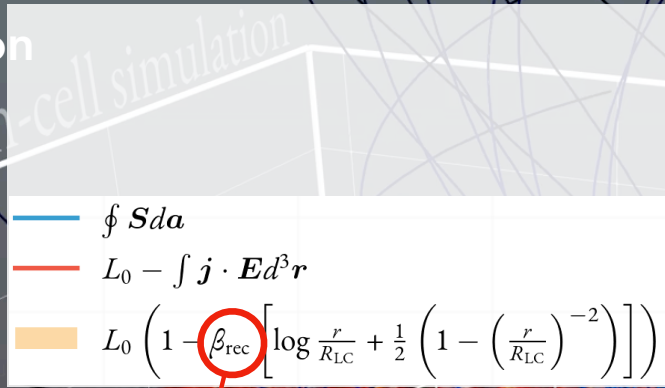
# Energy dissipation (dependence on the inclination & cooling strength)



1. cooling strength **does not affect** the dissipation (reconnection) rate;
2. larger inclinations have displacement current  
 $\Rightarrow$  weaker resistive current  
 $\Rightarrow$  **less dissipation**

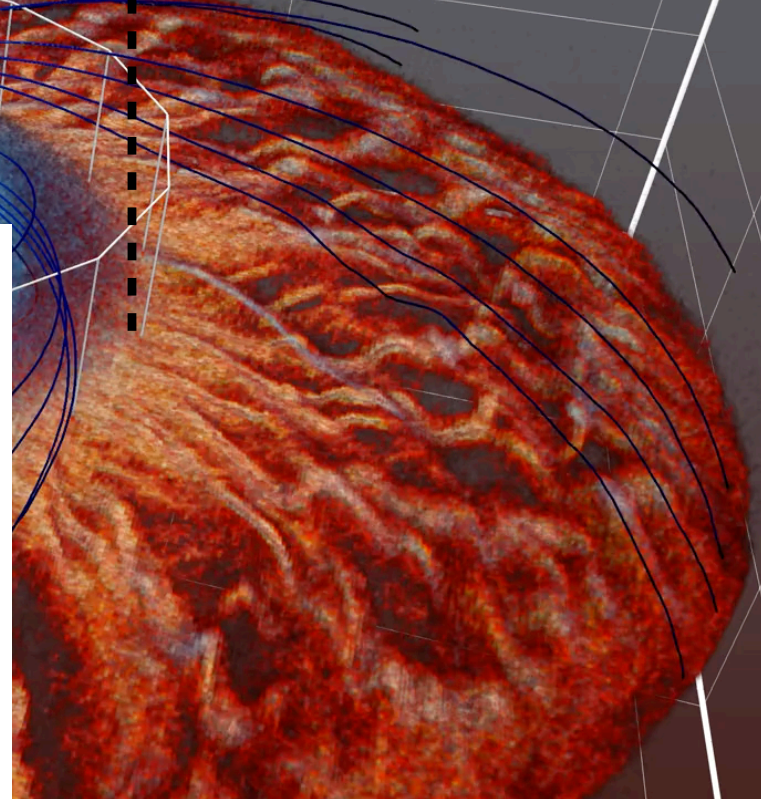
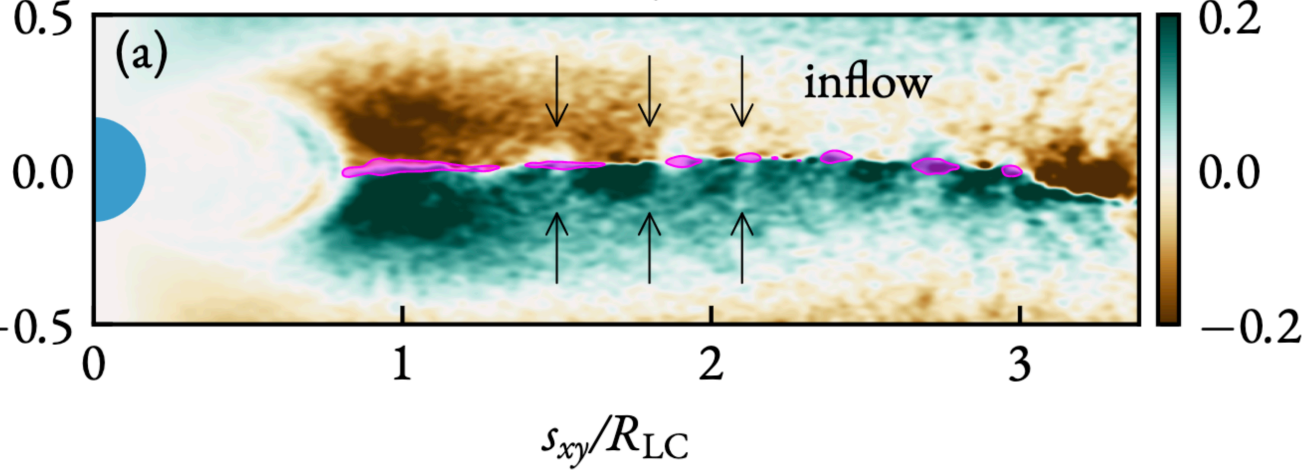
# Energy dissipation

Particle-in-cell simulation



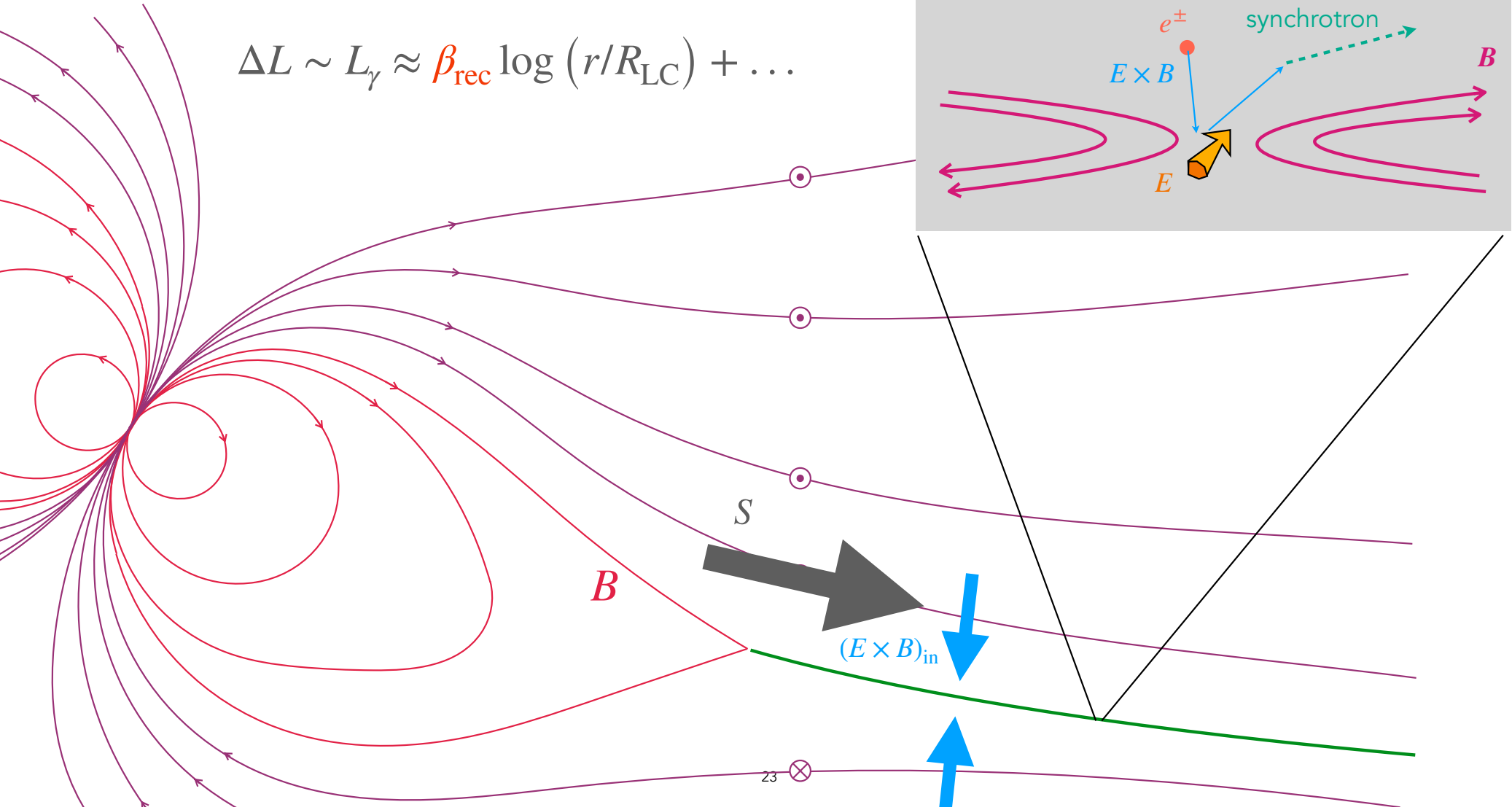
**prediction:** about 1-10% is dissipated within the first  $R_{\text{LC}}$

$$\beta_{\text{rec}} \equiv (\mathbf{E} \times \mathbf{B})_z / |\mathbf{B}|^2$$



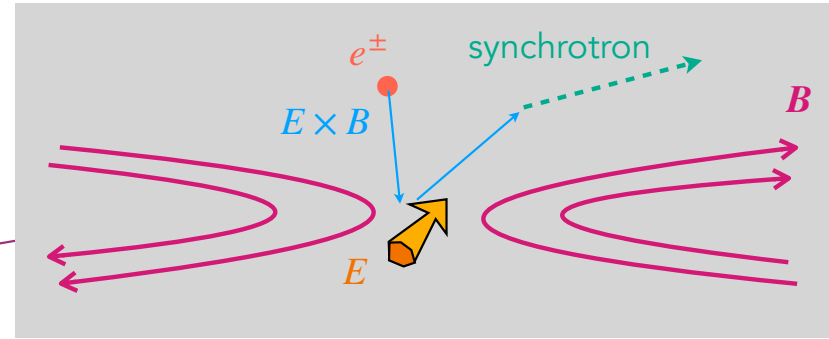
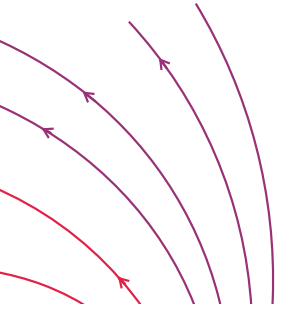
# Reconnection-driven Poynting flux dissipation

$$\Delta L \sim L_\gamma \approx \beta_{\text{rec}} \log(r/R_{\text{LC}}) + \dots$$



# Reconnection-driven Poynting flux dissipation

$$\Delta L \sim L_\gamma \approx \beta_{\text{rec}} \log(r/R_{\text{LC}}) + \dots$$

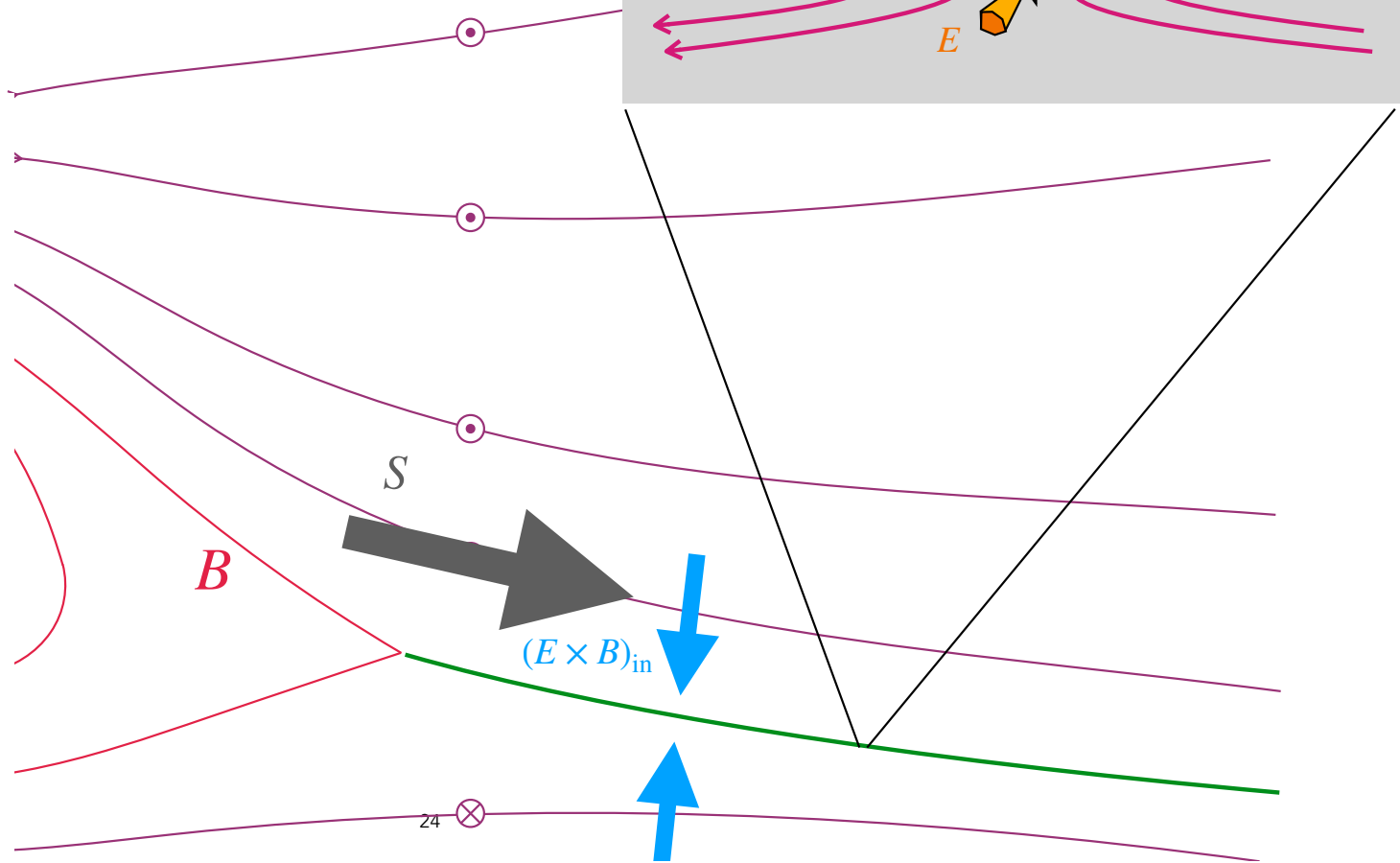


collisionless reconnection rate is **universal**:

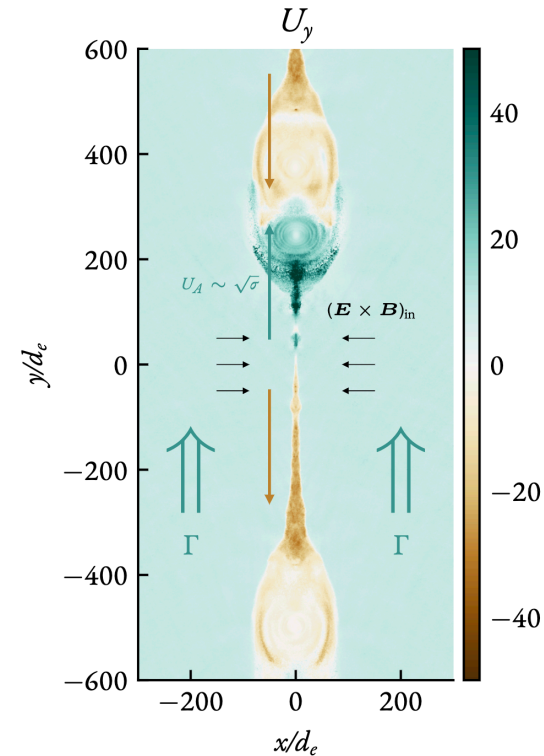
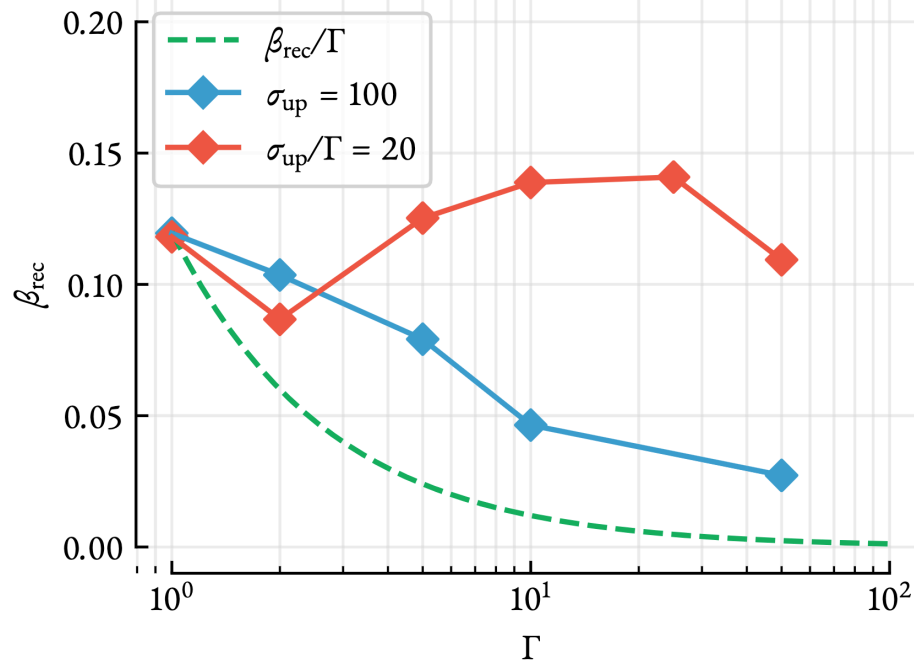
$$\beta_{\text{rec}} \approx 0.1 v_A \approx 0.1 c$$

key assumptions:

- $\sigma \gg 1$
- $\Gamma_{\text{bulk}} \lesssim \sqrt{\sigma}$
- $d_e \ll \rho_G \ll R_{\text{LC}}$
- [^] asymptotic regime (large scale separation)



**Puzzle: reconnection rate in the lab frame is 0.1 independent of upstream flow boost**

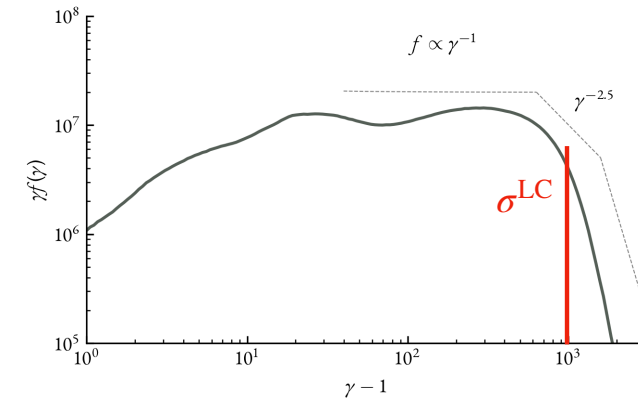
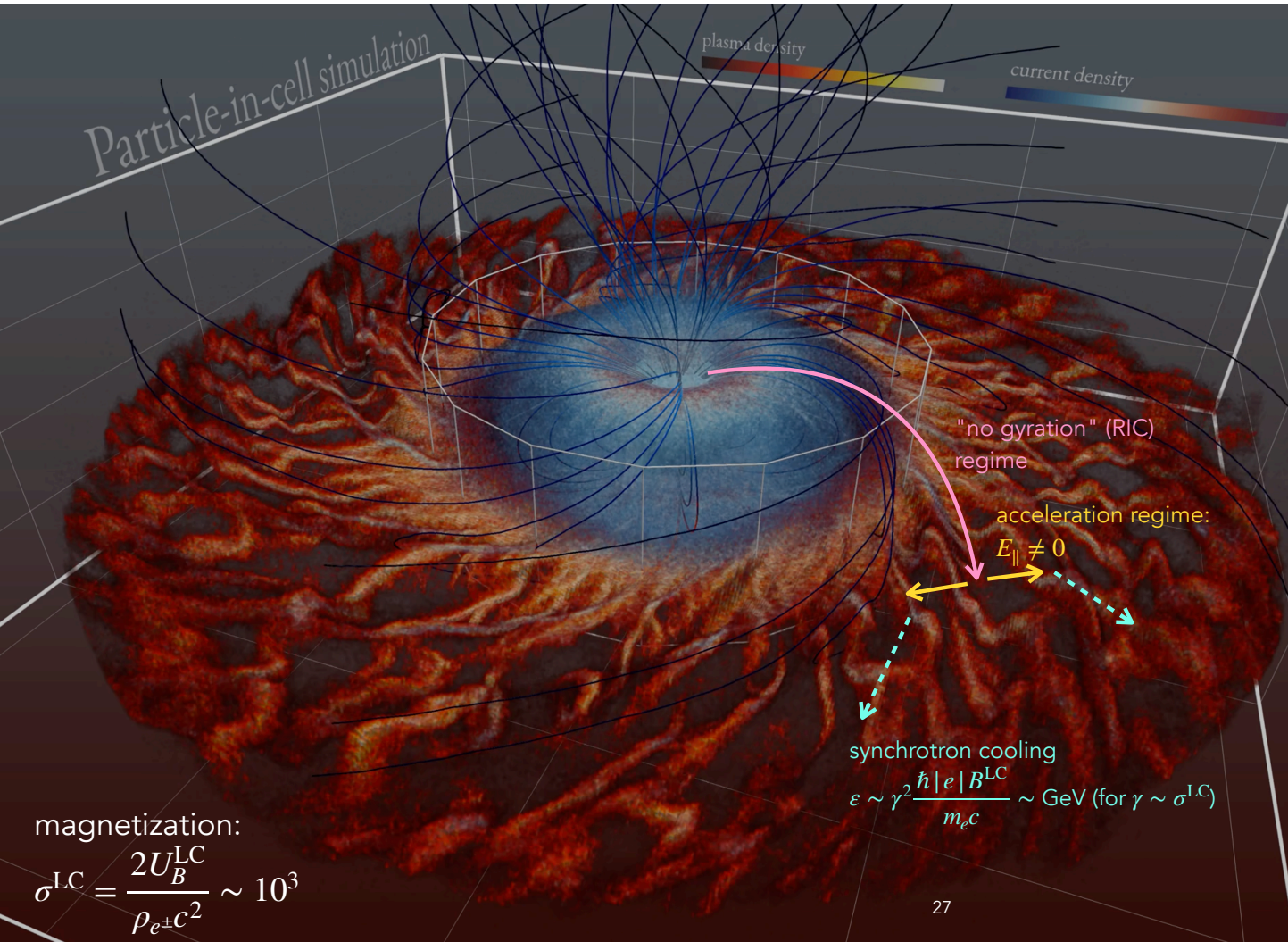


**Simulation of reconnection rate in a setup with boosted upstream:  
Physics cares about x-points which are still stationary in the lab frame if  
gamma of flow < sqrt(sigma)**

## Takeaways

- Microscopic kinetic instability (magnetic reconnection) powers the Poynting flux dissipation of pulsar magnetospheres;
- about 0.1-10% of the spindown power is dissipated (within the few  $R_{LC}$ );
- this fraction only depends on the inclination angle  $\chi$  and is insensitive to plasma parameters and cooling strength;
- reconnection accelerates particles up to  $E \sim \sigma^{LC} m_e c^2$  (no matter the cooling strength);  $\gamma$ -ray emission is produced via synchrotron mechanism.

# Particle acceleration and photon emission

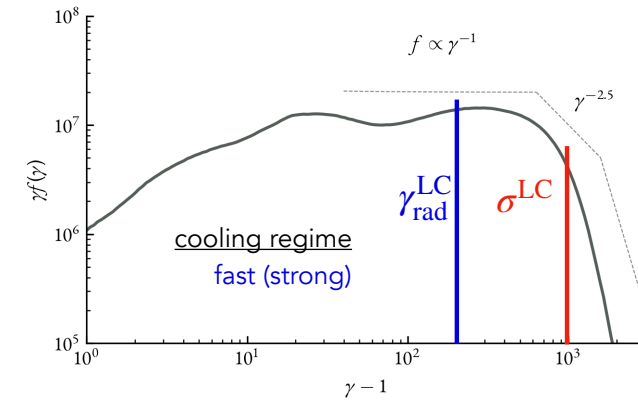
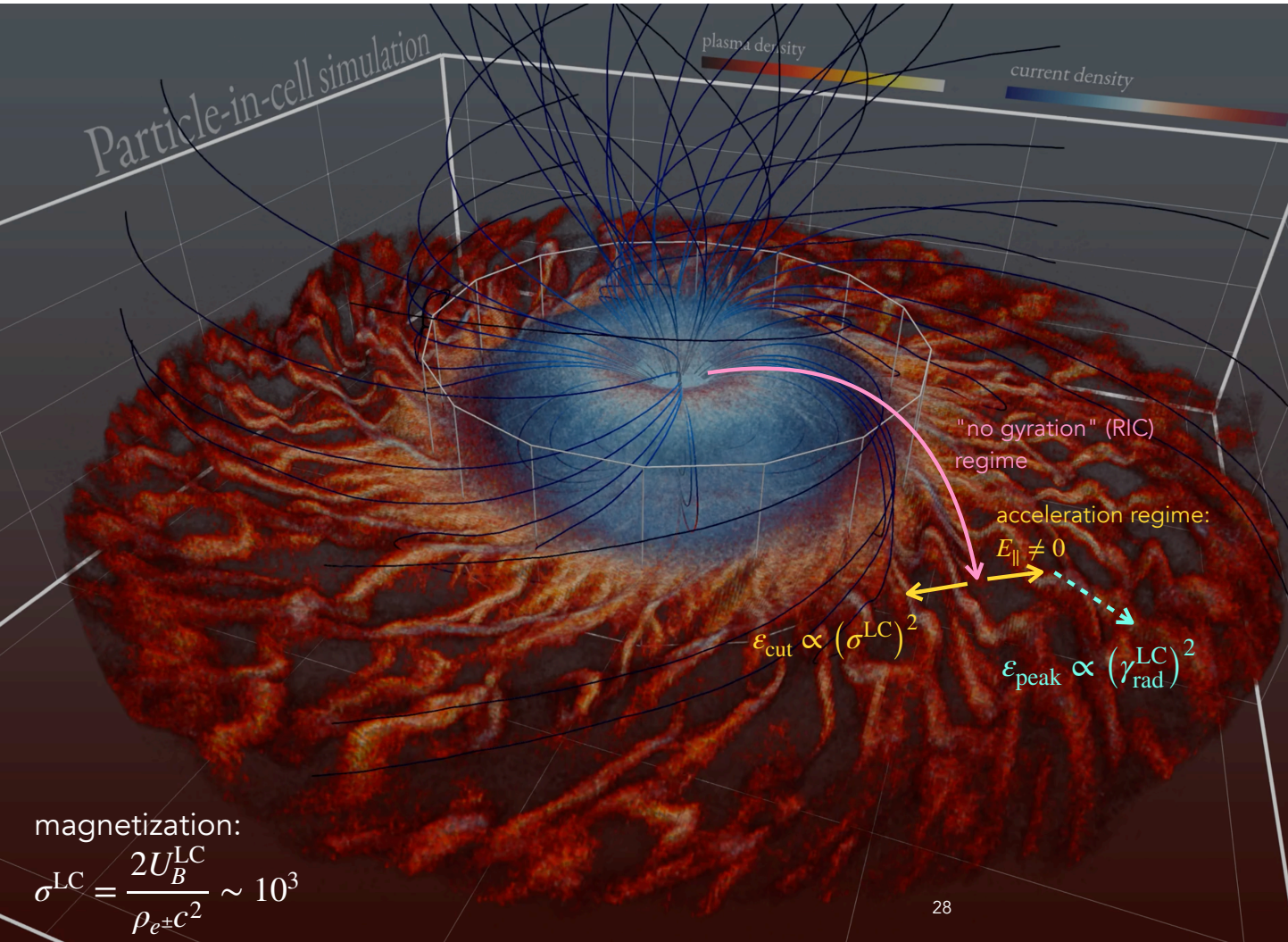


Strength of synchrotron cooling vs acceleration in reconnection:

$$|e| E_{\text{rec}}^{\text{LC}} = \sigma_T U_B^{\text{LC}} (\gamma_{\text{rad}}^{\text{LC}})^2$$

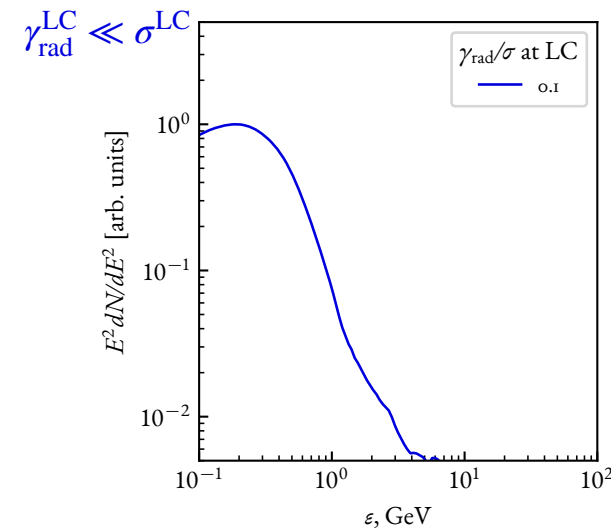
$$\gamma_{\text{rad}}^{\text{LC}} \sim 10^5 (B_{\text{LC}}/10^5 \text{ G})^{-1/2}$$

# Particle acceleration and photon emission

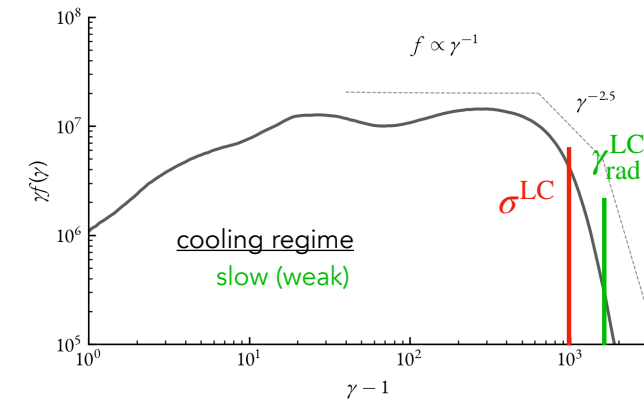
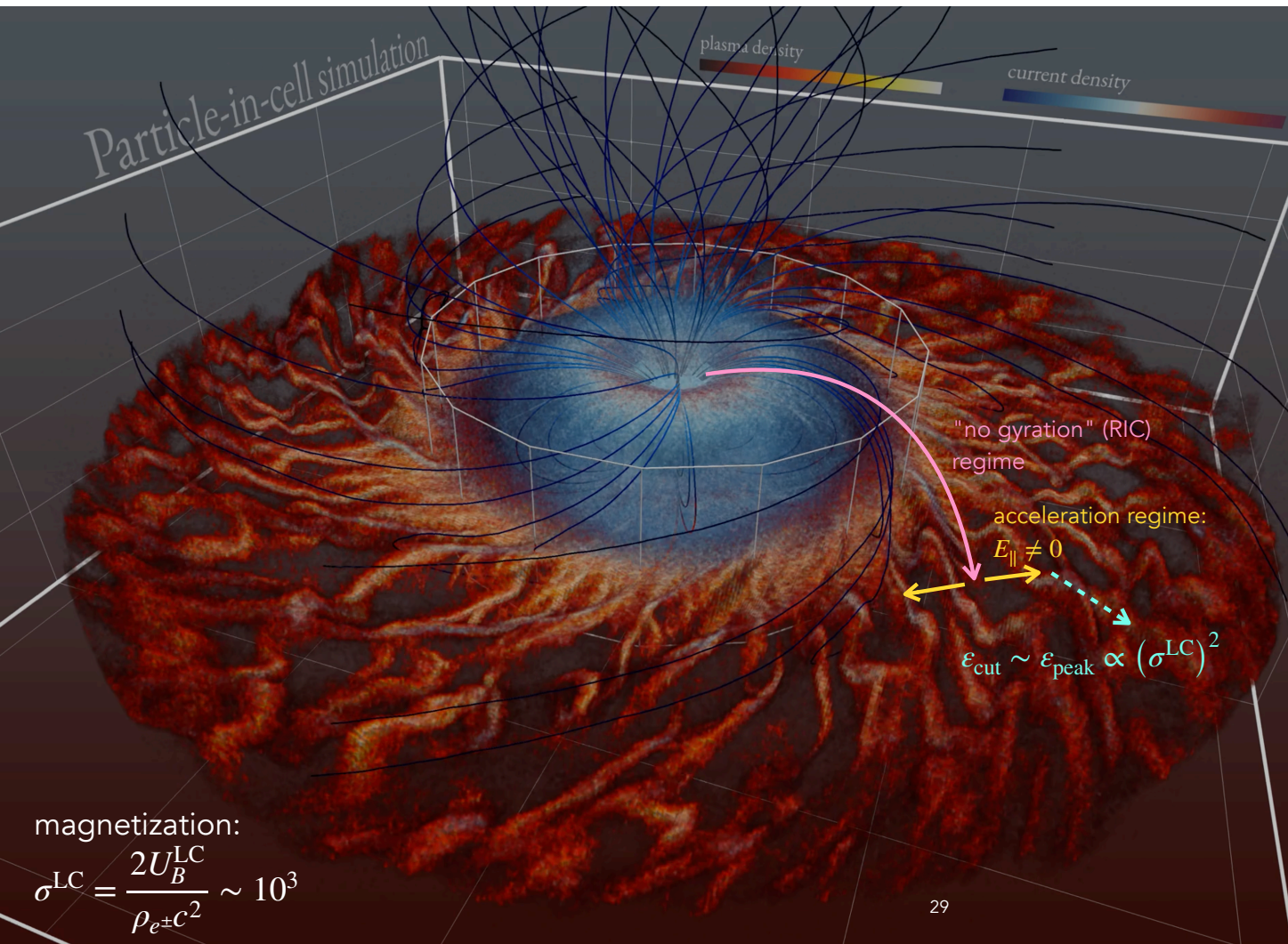


Strength of synchrotron cooling vs acceleration in reconnection:

$$|e| E_{\text{rec}}^{\text{LC}} = \sigma_T U_B^{\text{LC}} (\gamma_{\text{rad}}^{\text{LC}})^2$$

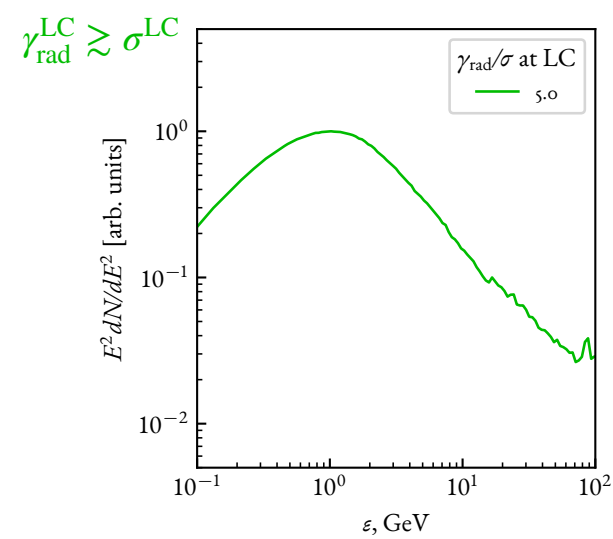


# Particle acceleration and photon emission

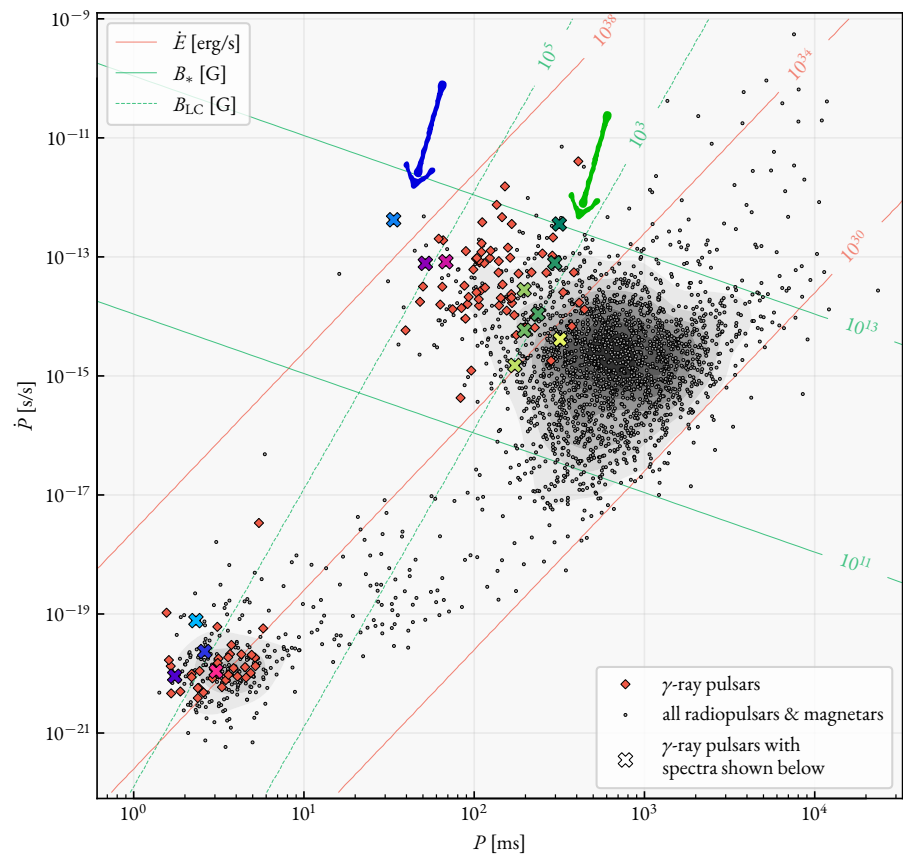


Strength of synchrotron cooling vs acceleration in reconnection:

$$|e| E_{\text{rec}}^{\text{LC}} = \sigma_T U_B^{\text{LC}} (\gamma_{\text{rad}}^{\text{LC}})^2$$

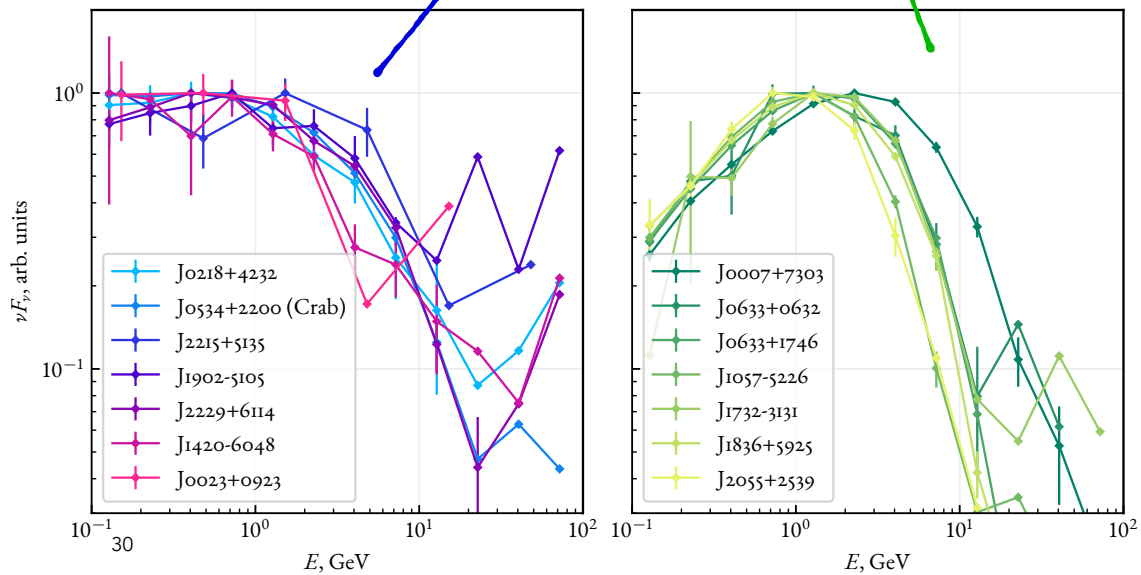
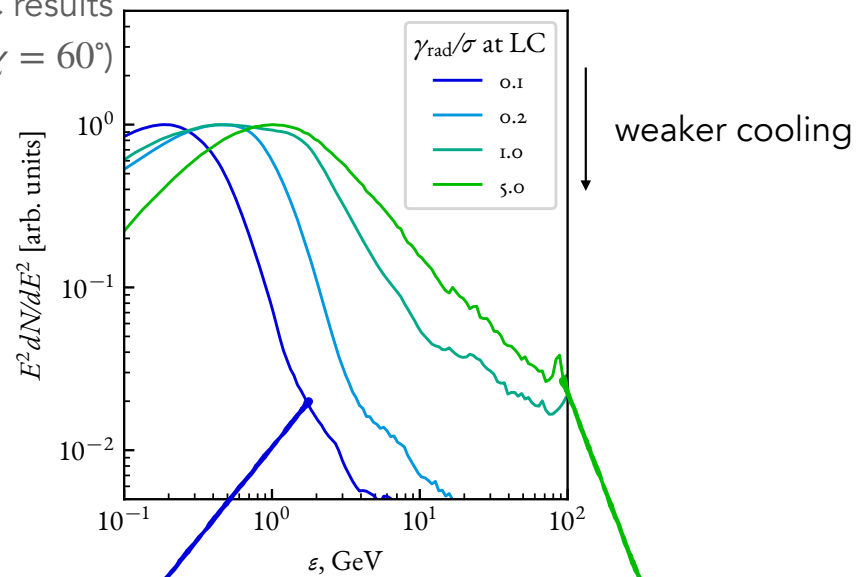


# Dichotomy in $\gamma$ -ray pulsar spectra



PIC results

( $\chi = 60^\circ$ )



# Effect of cooling strength on spectra of particles and photons: 2D

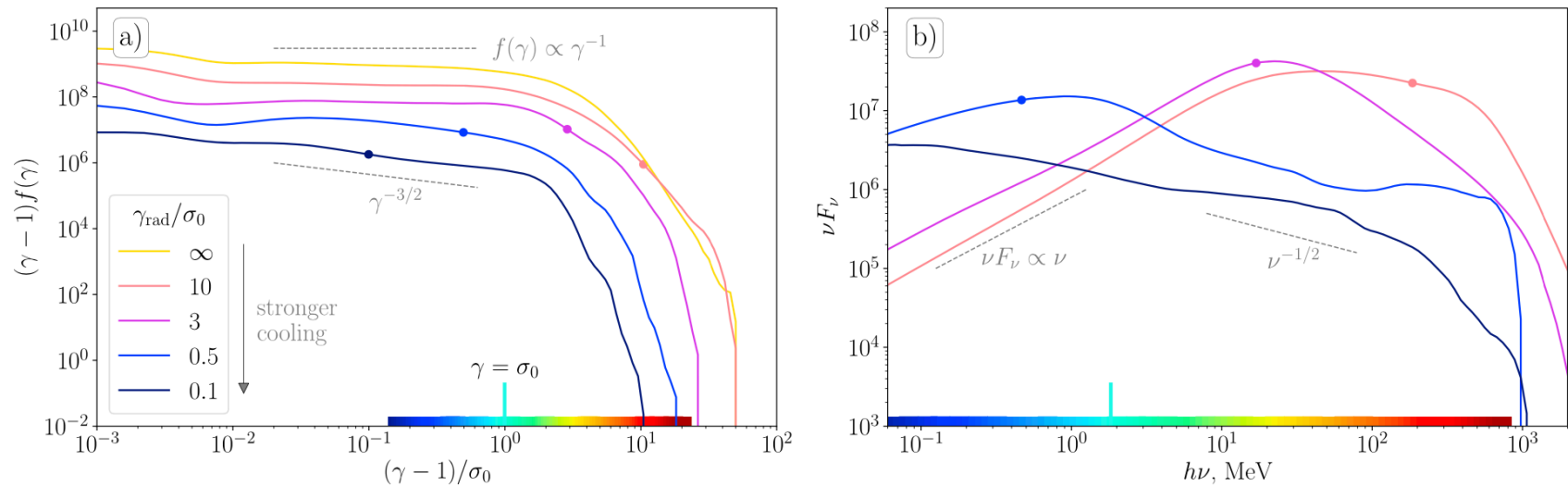


**Figure 9.** Particle and photon spectra for the  $\sigma_0 = 200$  simulations without pair production for different cooling regimes in late-time steady state. The cooling decreases (i.e.,  $\gamma_{\text{rad}}$  increases) from dark blue to yellow;  $\gamma_{\text{rad}} = \infty$  is the case without cooling (i.e., no photons). Two colorbars below put particle energies and synchrotron photon energies into correspondence, given a fixed background magnetic field, which in general varies depending on particle position. Particle spectra are shifted vertically for illustration purposes; circles indicate  $\gamma_{\text{rad}}$  for each case, as well as the corresponding synchrotron photon energy in the upstream magnetic field. Cooling typically conserves the  $\gamma^{-1} - \gamma^{-3/2}$  slope of the particle energy distribution function. Peaks in synchrotron photon spectra for each case corresponding to  $\gamma_{\text{rad}}$  in particles; high-energy tails with  $\nu F_\nu \propto \nu^{-1/2}$  are formed during transient mergers, when particles accelerated in secondary current sheets are captured by plasmoids and rapidly cooled.

# Effect of cooling strength on spectra of particles and photons: 3D

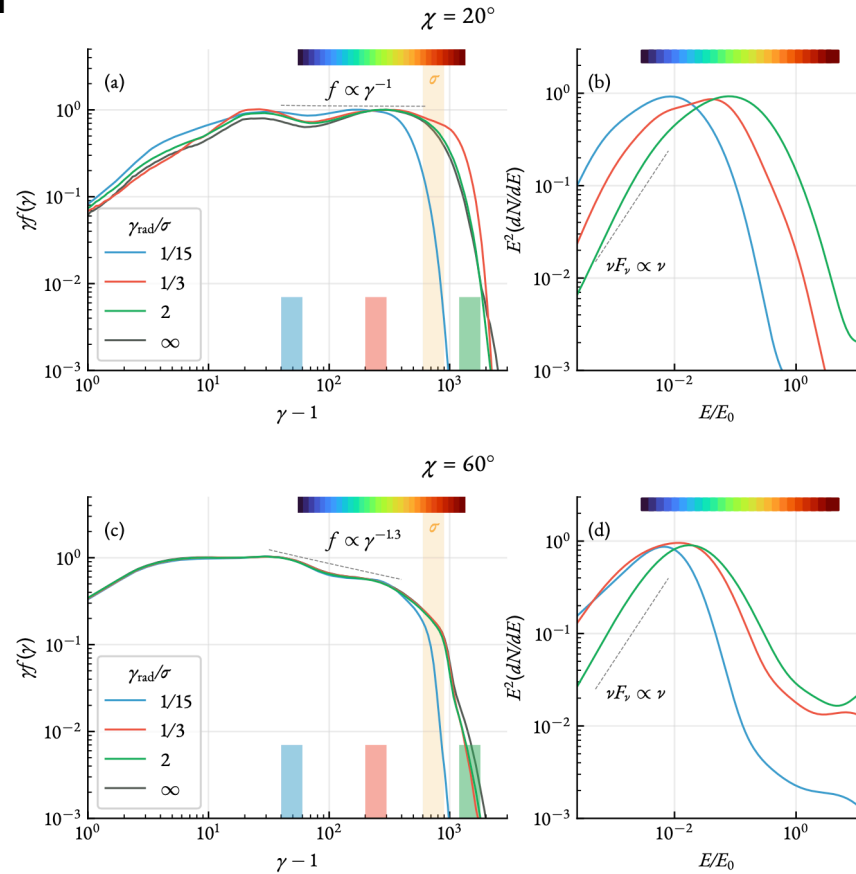
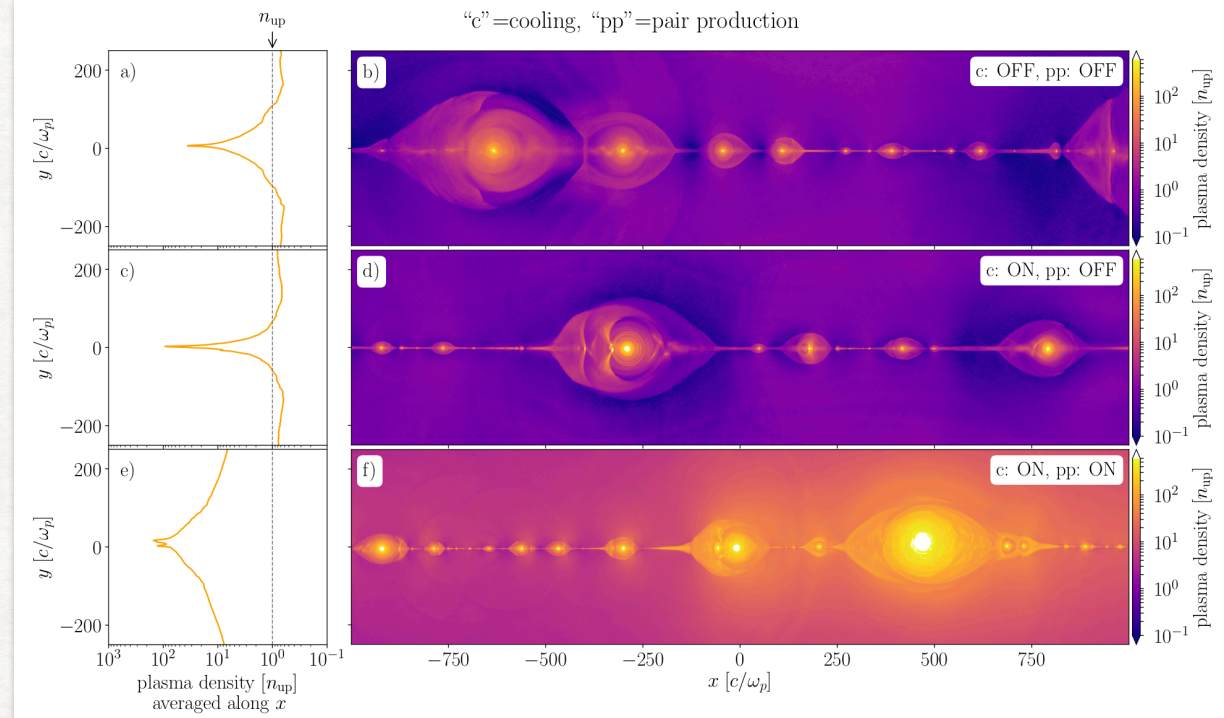
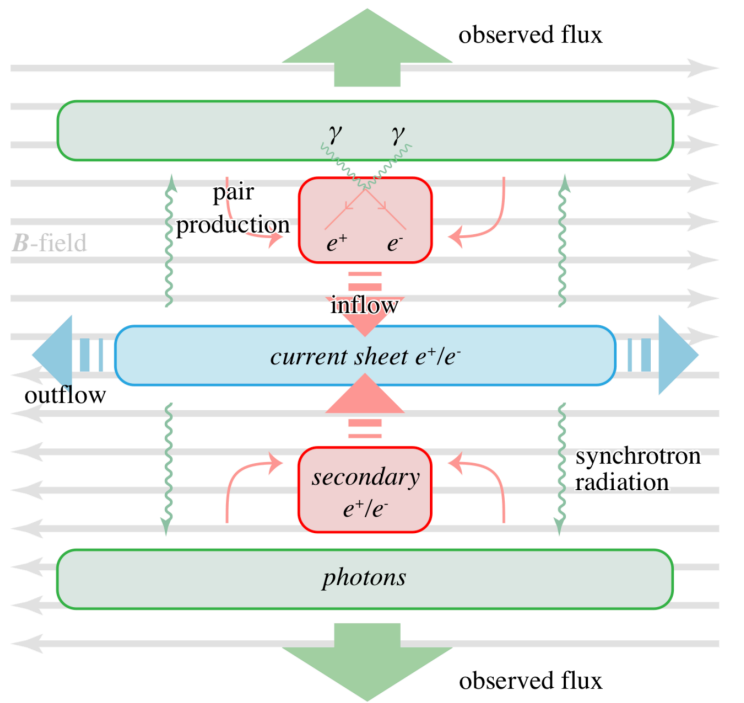


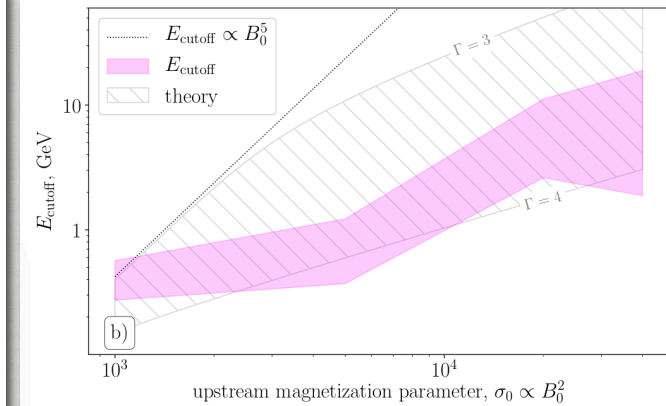
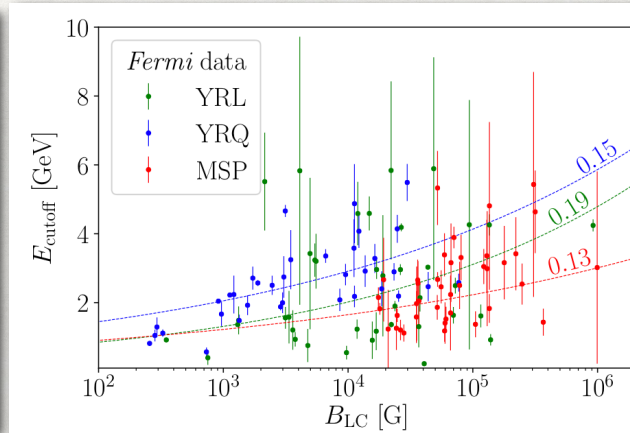
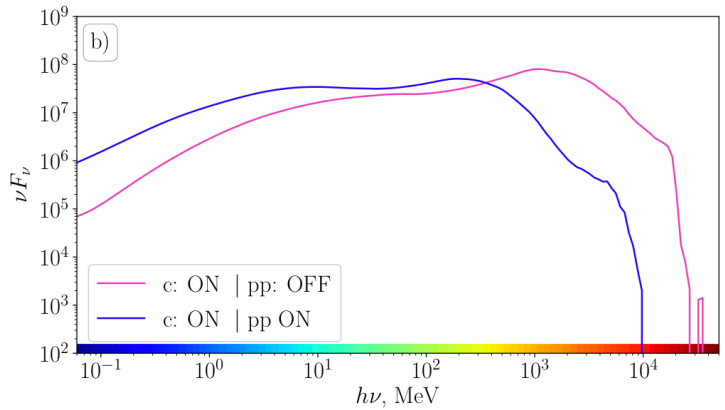
**Figure 8.** (a, c) particle and (b, d) photon spectra for the R75\_ang20, and R75\_ang60 simulations in different synchrotron cooling regimes. Effective  $\sigma$  at the light cylinder is marked with yellow stripes. Three smaller bars of different colors in (a) and (c) indicate the effective  $\gamma_{\text{rad}}$ . Colorbar at the top of both panels puts particle peak energies into correspondence with synchrotron peak energies,  $E \propto \gamma^2 B_{\text{LC}}$ . Photon energies are normalized to  $E_0 \propto (\sigma^{\text{LC}})^2 B_{\text{LC}}$ . While particle spectra look almost identical (except for the strongest cooled case), peaks of photons are shifted to smaller energies for smaller  $\gamma_{\text{rad}}/\sigma$ . Only particles in the current layer are accounted for. Simulations without synchrotron cooling (black lines) are not shown in panels (b) and (d), since we do not collect photons in that case.

# THE ROLE OF RECONNECTION WITH PAIR PRODUCTION IN SETTING CUTOFF ENERGY



Reconnection in the current sheet is the main particle accelerator. Gamma-gamma pair formation can start and increases the pair loading above the sheet, lowering effective magnetization in the sheet. Particle acceleration follows magnetization, max particle energy is reduced. This results in weaker dependence of maximum gamma-ray energy on the magnetic field at the light cylinder than would be naively expected.

# THE ROLE OF RECONNECTION WITH PAIR PRODUCTION IN SETTING CUTOFF ENERGY



Pair formation increases the pair loading above the sheet, and lowers effective magnetization in the sheet. Particle acceleration follows magnetization, max particle energy is reduced. Synchrotron emission. Naively, cutoff energy should be a strong function of B at the LC.

$$\gamma_{\text{cutoff}} \propto \sigma_0 \propto B_0^2, \quad E_{\text{cutoff}} \propto \gamma_{\text{cutoff}}^2 B_0 \propto B_0^5$$

Pair loading softens the dependence

$$\gamma_{\text{cutoff}} \sim \sigma_{\text{LC}} \propto B_{\text{LC}}^2 / \eta n_{\text{GJ}}$$

Expect cutoff energy dependence to be between  $E_{\text{cutoff}} \propto B_{\text{LC}}^{1.2} - B_{\text{LC}}^{1.8}$  and  $E_{\text{cutoff}} \propto B_{\text{LC}}^{-0.8} - B_{\text{LC}}^{-0.2}$

Observed dependence:

$$E_{\text{cutoff}} \propto B_{\text{LC}}^{0.1} - B_{\text{LC}}^{0.2}$$

# Effect of pair loading on spectra of particles and photons: 2D simulations

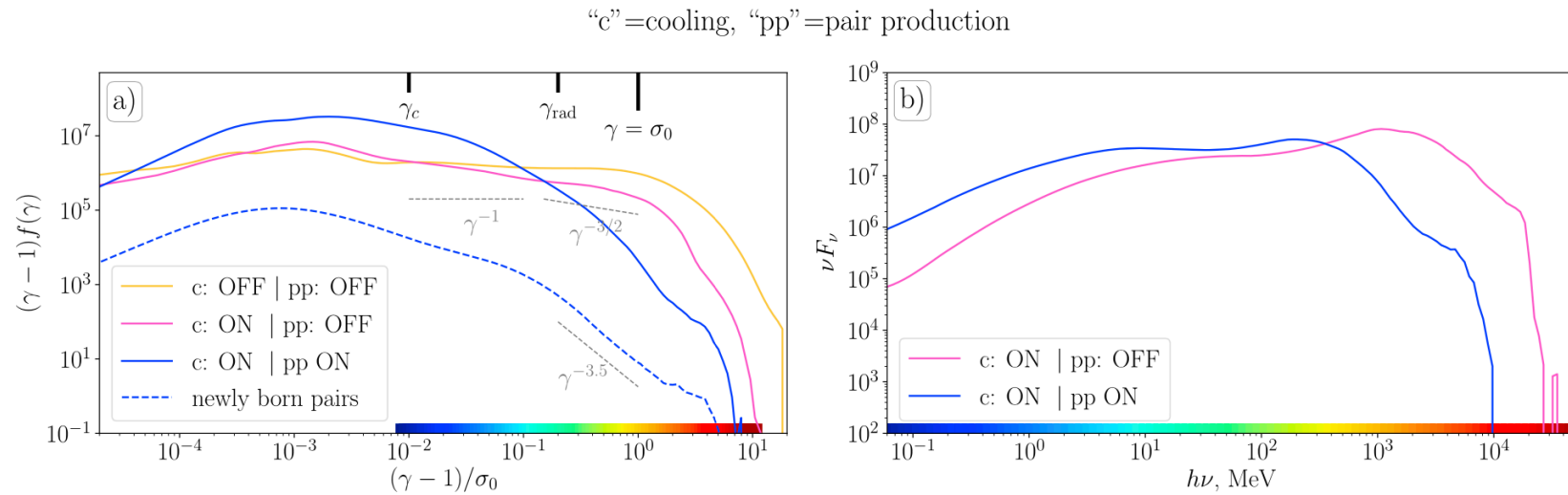


**Figure 10.** Particle (a) and photon (b) spectra for the  $\sigma_0 = 5000$ ,  $\gamma_{\text{rad}} = 1000$ ,  $\gamma_c = 50$  simulations without cooling, with cooling but without pair production, and with both cooling and pair production enabled in late-time steady state. Two colorbars below put particle energies and synchrotron photon energies into correspondence, given a fixed background magnetic field. Dashed line is the spectrum of newly born secondary pairs in the run with pair production. Cooling does not strongly affect the slope, whereas when pair production is enabled the effective magnetization is dropped, and the upstream is no longer cold (see the newly born pairs). This causes the shift of the peak in photon spectrum (corresponding to the effective magnetization,  $\sigma_{\text{eff}}$ ).

# Effect of pair loading on spectra of particles and photons: 3D simulations

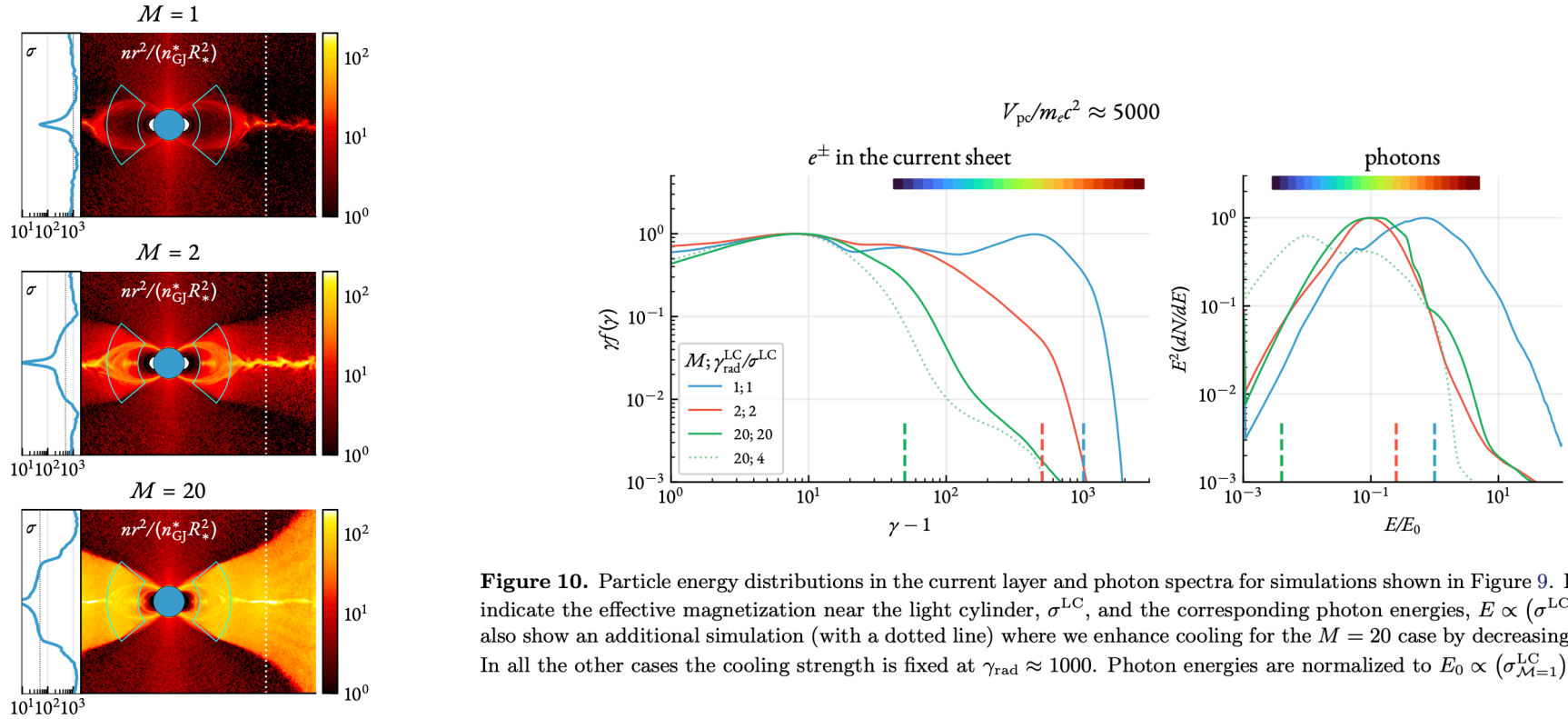


**Figure 9.** Three simulations R75\_ang0 with different pair loading rates. Additional injection region is highlighted with cyan. Newly created particles are initialized with zero velocity. From top to bottom,  $M = 1$  (no extra injection, all particles originate at the surface),  $M = 2$  (one particle is injected per each surface-injected particle),  $M = 20$ . To the left of each panel we plot the magnetization of the steady-state solution for each case as a function of vertical coordinate (corresponding slice is shown with a white dashed line).

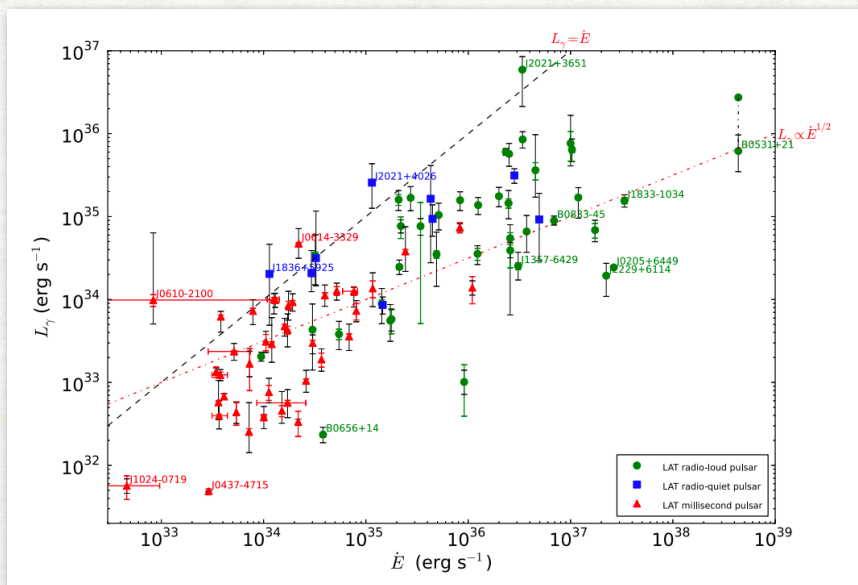
**Figure 10.** Particle energy distributions in the current layer and photon spectra for simulations shown in Figure 9. Dashed lines indicate the effective magnetization near the light cylinder,  $\sigma^{\text{LC}}$ , and the corresponding photon energies,  $E \propto (\sigma^{\text{LC}})^2 B_{\text{LC}}$ . We also show an additional simulation (with a dotted line) where we enhance cooling for the  $M = 20$  case by decreasing  $\gamma_{\text{rad}} \approx 200$ . In all the other cases the cooling strength is fixed at  $\gamma_{\text{rad}} \approx 1000$ . Photon energies are normalized to  $E_0 \propto (\sigma_{M=1}^{\text{LC}})^2 B_{\text{LC}}$ .

Cutoff of the particle spectrum is determined by effective magnetization at LC  
 Mass loading decreases magnetization  
 Peak of the spectrum is controlled by gamma-rad

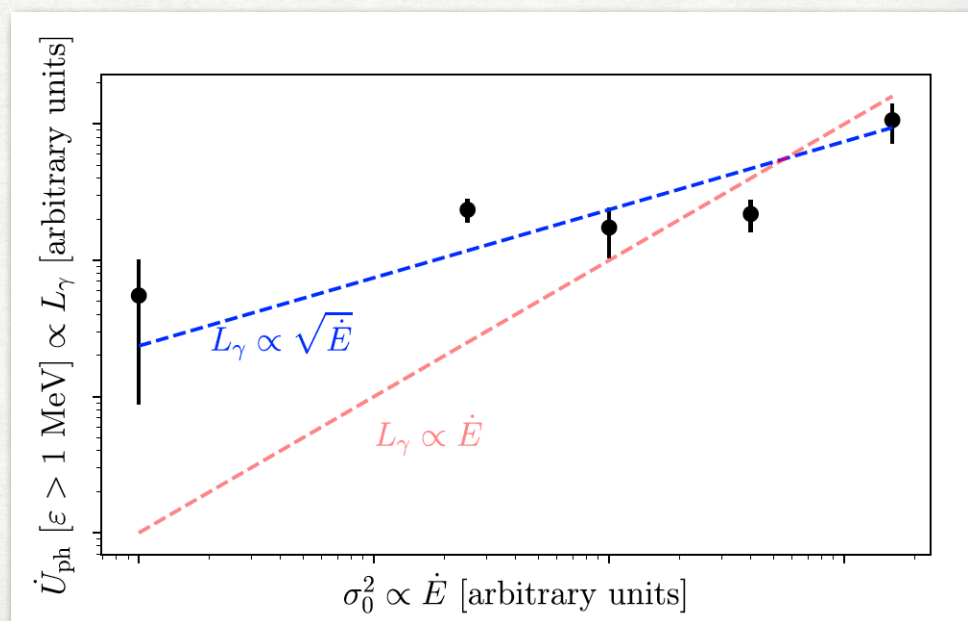
# THE ROLE OF RECONNECTION WITH PAIR PRODUCTION IN SETTING $L_\gamma$

Gamma luminosity is larger for aligned rotators than for oblique ones.  $L_\gamma/\dot{E}$  varies from 1% for orthogonal rotator to 10% for near aligned. Obliqueness effects can explain the spread in observed values of  $L_\gamma$ . In this regime  $L_\gamma \propto \dot{E}$ .

Pair formation in the current sheet decreases magnetization and lowers maximum particle energy, and radiative efficiency decreases. This leads to slower Edot dependence.



Abdo et al 2013



Hakobyan, Philippov, AS 2019 16

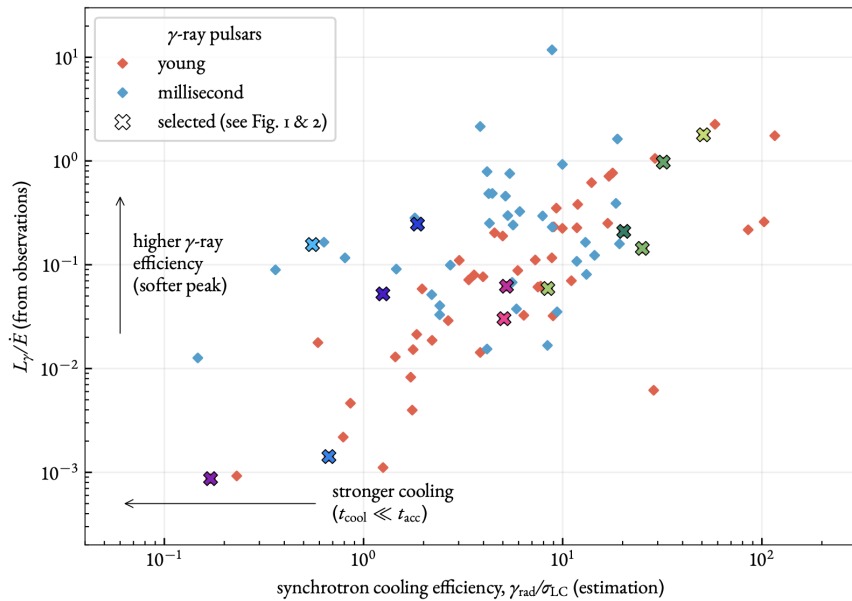
# [\*] Pair-loading of the current sheet

How large the multiplicity,  $\kappa$ , can become (w.r.t. GJ):<sup>[1]</sup>

$$\kappa \approx 2 \cdot 10^6 \left( \frac{\dot{E}}{10^{38} \text{ erg/s}} \right)^{3/2} \left( \frac{P}{100 \text{ ms}} \right)^{-1} \left( \frac{L_X/\dot{E}}{0.1 \%} \right) \left( \frac{L_\gamma/\dot{E}}{10 \%} \right)$$

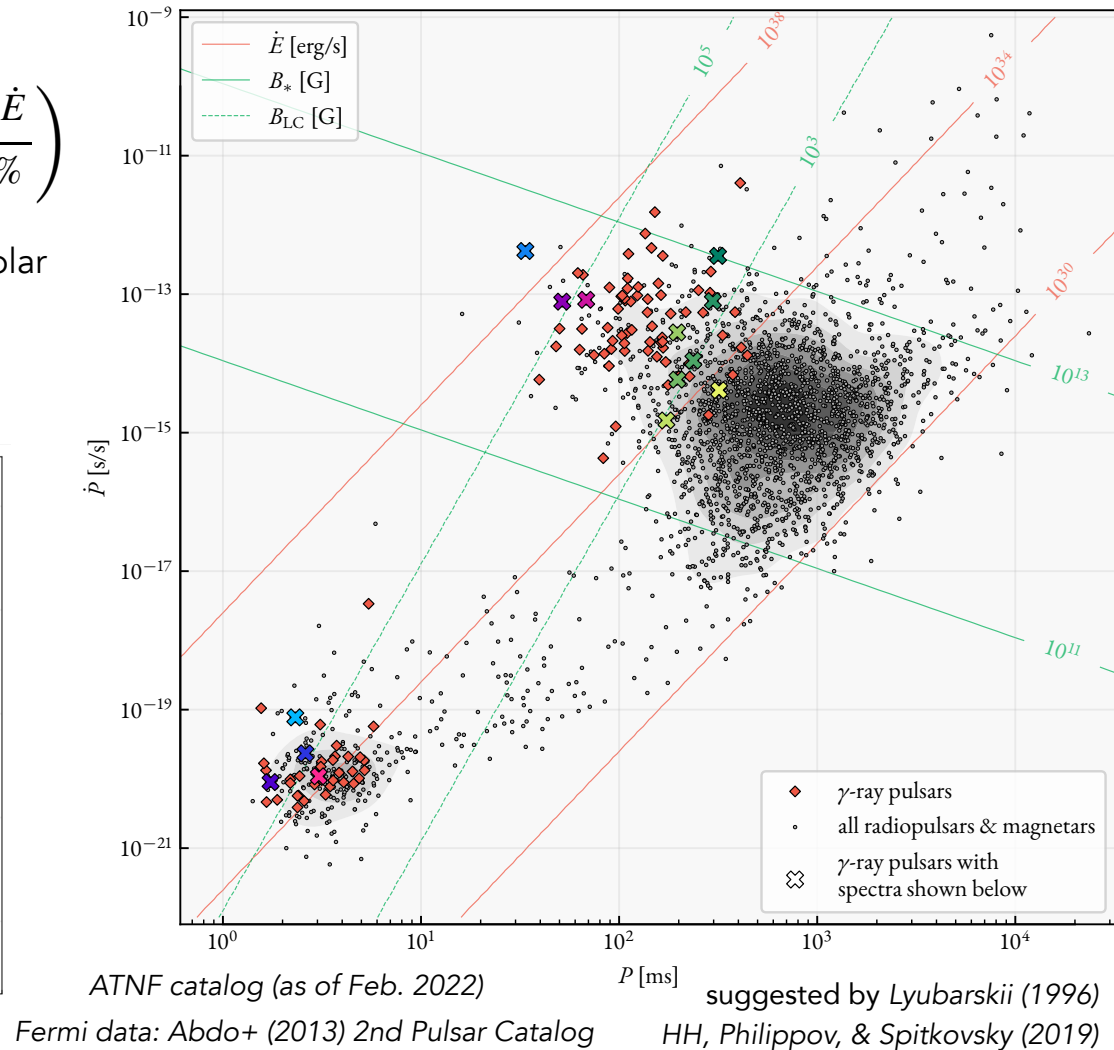
For Crab pulsar  $n_{\gamma\gamma}/n_{\text{GJ}} \sim 10^7$  (compare with  $10^4$  that the polar cap can provide), for Vela  $\sim 10$ .<sup>[2]</sup>

$$\sigma_{\text{LC}}^{\text{LC}} \sim \frac{\omega_B}{2\Omega} \frac{1}{\kappa} \quad \gamma_{\text{rad}}^{\text{LC}} \sim 10^5 (B^{\text{LC}}/10^5 \text{ G})^{-1/2}$$



[1] Philippov (private blackboard comm., ~2021)

[2] Lyubarskii (1996)



## Conclusions

- Reconnection leads to **dissipation of 0.1-10% of the spindown power** (within the few  $R_{LC}$ );
- Cooling strength at LC controls the shape of the spectrum ( $\gamma_{rad}/\sigma$ ).
- Sigma at LC (pair production or plasma supply from surface) controls max particle energy.
- Low  $\dot{E}$  pulsars have weak pair production at LC
- High  $\dot{E}$  pulsars — strong pair production at LC. Secondary pairs will re-radiate the energy at lower photon energy — MeV/keV pulsars?
- $L_\gamma/\dot{E}$  is lower for high  $\dot{E}$  pulsars because secondary pairs remove the energy to lower energy photons
- Combination of  $\gamma_{rad}$  and pair loading is responsible for weak dependence of cutoff energy in photons with magnetic field.